



CHALMERS
UNIVERSITY OF TECHNOLOGY

From Low-Loaded Mesophilic to High-Loaded Thermophilic Anaerobic Digestion: Changes in Reactor Performance and Microbiome

Downloaded from: <https://research.chalmers.se>, 2026-04-21 17:26 UTC

Citation for the original published paper (version of record):

Modin, O., Zheng, D., Schnürer, A. et al (2025). From Low-Loaded Mesophilic to High-Loaded Thermophilic Anaerobic Digestion: Changes in Reactor Performance and Microbiome. *Microbial Biotechnology*, 18(10).
<http://dx.doi.org/10.1111/1751-7915.70238>

N.B. When citing this work, cite the original published paper.

RESEARCH ARTICLE OPEN ACCESS

From Low-Loaded Mesophilic to High-Loaded Thermophilic Anaerobic Digestion: Changes in Reactor Performance and Microbiome

Oskar Modin¹  | Dan Zheng¹  | Anna Schnürer²  | Ted Lundwall³ | Santiago Elejalde Bolanos³ | Jesper Olsson³ ¹Division of Water Environment Technology, Architecture and Civil Engineering, Chalmers University of Technology, Gothenburg, Sweden | ²Department of Molecular Sciences, Swedish University of Agricultural Sciences, Uppsala, Sweden | ³The Käppala Association, Lidingö, Sweden**Correspondence:** Oskar Modin (oskar.modin@chalmers.se)**Received:** 30 April 2025 | **Revised:** 30 July 2025 | **Accepted:** 18 September 2025**Funding:** This study was supported by Käppalaförbundet and The Swedish Research Council (VR).**Keywords:** anaerobic digestion | metagenomics | methanogenesis | wastewater sludge treatment

ABSTRACT

This study investigated temporal dynamics in reactor performance and microbial community structure during anaerobic digestion of sewage sludge when the temperature was changed from 37°C to 55°C, followed by an increase in organic loading rate (OLR). Performance instability was observed immediately following the temperature increase and in the end of the study when the OLR was $11.1 \pm 0.3 \text{ kgVS m}^{-3} \text{ d}^{-1}$. The specific methane production peaked at $0.31 \pm 0.06 \text{ Nm}^3 \text{ kg}^{-1}$ volatile solids (VS) during thermophilic operation and when the OLR was $3.5 \pm 0.9 \text{ kgVS m}^{-3} \text{ d}^{-1}$. Using metagenomic sequencing, 304 species-representative genome bins (SGB) were assembled. Network analysis revealed that 186 SGB were associated with thermophilic conditions and several new species putatively involved in key reactor functions were identified. When reactor function initially stabilised, two hydrogenotrophic and one aceticlastic methanogen (*Methanothermobacter* spp. and *Methanosarcina thermophila*), the hydrolytic *Coprothermobacter proteolyticus*, and putative syntrophic propionate oxidisers (e.g., *Pelotomaculaceae*) had high relative abundance. During the peak in specific gas production, the community was dominated by one hydrogenotrophic *Methanothermobacter* species coexisting with syntrophic acetate oxidising bacteria (*Thermacetogenium phaeum* and other species). Finally, when the reaction function deteriorated due to high OLR, new hydrolytic taxa emerged and the same aceticlastic methanogen as seen during the initial acclimatisation phase returned.

1 | Introduction

Anaerobic digestion (AD) is commonly used to hygienise, minimise, and valorise sewage sludge (Kjerstadius et al. 2013; Zhang et al. 2017; Ferrer et al. 2024). In the process, a microbial community degrades complex organic matter and produces biogas, mainly consisting of methane and carbon dioxide. The digestion process is accomplished by several co-dependent functional groups of microorganisms (Narihiro et al. 2015; Zhang et al. 2023). The first step, hydrolysis, solubilises particulate organic substrates. It is considered the

rate-limiting step in the digestion of waste activated sludge (Appels et al. 2008) and is performed by both free and sludge-bound hydrolytic enzymes (Guo et al. 2021). The second step is acidogenic fermentation of amino acids, carbohydrates, and lipids into organic acids and alcohols. Butyrate, propionate, and acetate are typically major fermentation products (Bengtsson et al. 2008; Wang, Chen, and Chang 2024; Wang, Zhang, et al. 2024). In the third step, acetogenesis, the organic acids and alcohols are further degraded into mainly acetate, H₂, formate, and CO₂; and in the fourth step, methanogenesis, H₂/formate and CO₂ or acetate are converted into methane.

This is an open access article under the terms of the [Creative Commons Attribution-NonCommercial-NoDerivs](https://creativecommons.org/licenses/by-nc-nd/4.0/) License, which permits use and distribution in any medium, provided the original work is properly cited, the use is non-commercial and no modifications or adaptations are made.

© 2025 The Author(s). *Microbial Biotechnology* published by John Wiley & Sons Ltd.

Several other compounds including methanol, methylated amines, and methylated sulfur compounds may also be used by some methanogens (Kurth et al. 2020). The degradation of butyrate and propionate into acetate and H_2 /formate is only thermodynamically favourable at very low concentrations of the products. Syntrophy between propionate- or butyrate-oxidising bacteria and H_2 /formate consumers such as hydrogenotrophic methanogens is therefore important for the process to function (Liu et al. 2021). Acetate can be directly converted to methane by aceticlastic methanogens but under certain conditions, such as elevated ammonium and temperature, an alternative route via syntrophic acetate oxidation to H_2 /formate and CO_2 , in a next step used by hydrogenotrophic methanogens, becomes more important (Westerholm et al. 2016).

Temperature is a determining factor for both the performance and microbial community composition of anaerobic digesters (Zhang et al. 2022). Large-scale digesters treating sewage sludge are typically operated at either mesophilic ($\sim 35^\circ C$) or thermophilic ($\sim 55^\circ C$) conditions. A major advantage of thermophilic operation is that the hydrolysis rate is approximately twice as high in comparison to mesophilic operation (Ge et al. 2011). Thus, a mesophilic digester that is converted to thermophilic operation could in theory increase the sludge degradation and biogas yield, which in turn could allow treatment of a comparably larger mass flow of sludge and a shorter retention time. Another advantage of thermophilic operation is improved inactivation of microbial pathogens, including eukaryotes, bacteria, and viruses (Kato et al. 2003; Kjerstadius et al. 2013; Yang et al. 2024). However, thermophilic temperature also presents some operational challenges. For example, thermophilic digesters are less stable and more prone to suffer from ammonia inhibition and acidification (Labatut et al. 2014; Ryue et al. 2020). Ammonium is released during degradation of proteins and is in equilibrium with ammonia, which is inhibitory to the overall process. Aceticlastic methanogens are more prone to inhibition than syntrophs and hydrogenotrophic methanogens (Liu et al. 2024). The ammonium equilibrium shifts towards ammonia with increasing temperatures leading to thermophilic processes being more prone to having problems. Temperature and ammonia levels are both strong regulators of microbial community structure and diversity, which decrease with increasing values (Sun et al. 2015; Westerholm et al. 2017; Theuerl et al. 2018). Thermophilic conditions and/or high ammonia levels also influence the relative importance of different functional groups of microorganisms. For example, as mentioned above, syntrophic acetate oxidation coupled to hydrogenotrophic methanogenesis is often more prevalent compared to aceticlastic methanogenesis at high temperature and ammonia levels (Westerholm et al. 2016).

The start-up of a thermophilic anaerobic digester for treatment of sewage sludge is often carried out with mesophilic sludge, especially if such a digester is already existing at the wastewater treatment plant (WWTP) (Angelidaki et al. 2006; Shin et al. 2019). The transition of mesophilic sludge to thermophilic conditions leads to a drastic change in microbial community composition and typically a temporary drop in biogas production (Tian et al. 2015; Westerholm et al. 2018). Several strategies for the temperature change have been tested and a rapid and immediate increase appears to lead to faster recovery of reactor performance as compared to a successive transfer (Boušková

et al. 2005; Shin et al. 2019). However, the possible rate of temperature increase is in practice limited by the heating capacity of the digester (Tezel et al. 2014). If the reason for the temperature change is to increase treatment capacity, an increase in organic loading rate (OLR) will follow the transition to thermophilic conditions. Increased OLR is known to affect the concentration and composition of produced volatile fatty acids (Wijekoon et al. 2011; Liu et al. 2017) and the microbial community composition and structure (Xu et al. 2018; Mercado et al. 2022). A too high OLR can also lead to reactor failure (Nkuna et al. 2022). Previous studies on the effects of a transition from mesophilic to thermophilic operation and/or increased OLR on the anaerobic digester microbiome have typically focused on taxonomic composition and diversity analysed by sequencing of the 16S rRNA gene (Shin et al. 2019; Wu, Shan, et al. 2020; Wu, Lin, et al. 2020; Zhang et al. 2022) while studies of changes in the functional potential of the microbiome using genome-resolved metagenomics are lacking. Moreover, studying shifts in functional potential and microbial community structure in digesters treating sewage sludge is particularly relevant as its lower nitrogen content, compared to for example food waste, minimizes the confounding effects of elevated free ammonia. This enables a clearer assessment of the impacts of temperature and organic loading rate (OLR) transitions. Furthermore, it remains unclear whether the thermophilic taxa that emerge during the temperature transition phase are the same as those that finally dominate under thermophilic operation at optimal loading conditions.

In this study, we examined temporal changes in reactor function and microbial community composition in a thermophilic anaerobic digester started up from mesophilic sludge at a municipal WWTP. The reactor was monitored throughout both the thermal adaptation phase and a subsequent period of stepwise increases in organic loading rate (OLR), under conditions where free ammonia concentrations remained stable. This controlled setting enabled us to isolate the effects of temperature and loading on microbial and functional shifts. Shotgun metagenomic sequencing was used to obtain information about both taxonomic composition and functional potential of both bacteria and archaea in the reactor at 26 time points during the 300-day operational period. The functional analysis included different metabolic steps in the AD process, i.e., hydrolysis, anaerobic oxidation, sulphate reduction, and methanogenesis, which could be linked to reactor performance. The study provides insights into the ecological and metabolic restructuring of microbial communities during thermophilic adaptation and loading transitions in sewage sludge digesters.

2 | Experimental Procedures

2.1 | The Anaerobic Digester System

The semi-full scale digester system was set up at Käppala WWTP in Sweden and consisted of a buffer tank ($1.2 m^3$), a weighing tank ($0.4 m^3$), a digester ($5 m^3$), a gasholder, and a flare (Figure S1) (Lundwall 2021; Elejalde Bolanos 2022). A mixture of primary sludge (65% of substrate mass) and waste activated sludge (35% of substrate mass) was pumped from the main WWTP to the buffer tank. Part of the sludge mixture in the buffer tank was pumped to the digester via the weighing

TABLE 1 | Operational conditions.

Phase	Time	Event	OLR (kgVS m ⁻³ d ⁻¹)	HRT ^a (d)
1	Day 0–40	Temperature transition (37°C–55°C) and acclimatisation	0.7 ± 0.6	~38
2	Day 41–110	Acclimatisation	2.3 ± 0.1	~18.4
3	Day 111–159	Increased load	2.8 ± 0.4	~14.1
4	Day 160–201	Increased load	3.5 ± 0.9	~11.3
5	Day 202–236	Increased load	4.9 ± 0.4	~8.4
6	Day 237–264	Increased load	5.8 ± 0.5	~7.1
7	Day 265–288	Increased load	7.3 ± 0.5	~5.1
8	Day 289–300	Increased load	11.1 ± 0.3	~4.1

^aThe hydraulic retention time (HRT) approached this value at the end of the phase.

tank once per hour. The weighing tank enabled precise measurements of the mass of substrate fed to the digester. The total solids (TS) content in the sludge was 5.2% ± 0.3% and the volatile solids (VS) fraction of the TS was 81% ± 2%. The total organic carbon content was 22.0–24.4 g L⁻¹, the total nitrogen content was about 2.4–2.8 g L⁻¹, and the total fat content was 5.2–7.3 g L⁻¹.

2.2 | The Experimental Campaign

The experimental campaign was divided into 8 phases (Table 1). Phase 1 was the temperature transition from mesophilic to thermophilic conditions, which was accomplished by a linear temperature increase from 37°C to 55°C over a period of 7 days. This phase also included an initial period with low OLR at the target temperature for 34 d to avoid overloading the reactor during acclimatisation of the sludge to thermophilic conditions. In Phase 2, the OLR was increased to 2.3 ± 0.1 kgVS m⁻³ d⁻¹, which is similar to the OLR of the full-scale mesophilic digester at the WWTP. This OLR was maintained for three hydraulic retention times (HRT). In Phases 3–8, the OLR was gradually increased to 11.1 ± 0.3 kgVS m⁻³ d⁻¹, which corresponded to a successive decrease in HRT to about 4.1 d. The increases in OLR were done in increments over a period of 7 days to avoid overloading the digester. Two exceptions were the change from Phases 6 to 7, which was done in increments over 14 days, and the change from Phases 7 to 8, which was done in one step. In each phase, the OLR level was maintained for at least three HRTs, except Phase 8, which was slightly shorter (see Table 1).

2.3 | Calculations

The HRT was calculated dynamically using the approach for solids retention time by Takács et al. (2008). The mesophilic anaerobic digester used to inoculate the thermophilic pilot reactor had an HRT of 18 days. Therefore, the starting HRT was set at 18 days and then the HRT was approximated recursively for each day of the experiment using Equation (1).

$$\text{HRT}_{t+\Delta t} = \text{HRT}_t + \Delta t \cdot \left(1 - \frac{Q \cdot \text{HRT}_t}{V}\right) \quad (1)$$

HRT_t is the HRT at time *t* (d), Δ*t* is the recursion time step (i.e., 1 day), *Q* is the flow (m³ d⁻¹), and *V* is the volume of the reactor (m³).

The OLR is the mass of added organic material (i.e., kg VS) per cubic meter of the reactor and per day. OLR was calculated using Equation (2).

$$\text{OLR} = \frac{Q \cdot \text{TS}_{\text{IN}} \cdot \text{VS}_{\text{IN}}}{V} \quad (2)$$

Q is the daily flow of sludge (m³ d⁻¹), TS_{IN} is the dry matter of the sludge (kgTS m⁻³) fed to the reactor, VS_{IN} is the organic fraction of the dry matter (kgVS kg⁻¹TS), and *V* is the volume of the digester (5 m³).

The VS removal efficiency was calculated using Equation (3).

$$\text{RE}_{\text{VS}} = 100\% \cdot \left(\frac{\text{TS}_{\text{IN}} \cdot \text{VS}_{\text{IN}} - \text{TS}_{\text{E}} \cdot \text{VS}_{\text{E}}}{\text{TS}_{\text{IN}} \cdot \text{VS}_{\text{IN}}}\right) \quad (3)$$

RE_{VS} is the VS removal efficiency (%), TS_E is the dry matter of the sludge in the reactor effluent, and VS_E is the organic fraction of the dry matter in the effluent.

The free ammonia concentration was calculated using Equation (4).

$$\text{FAN} = \frac{\text{TAN}}{1 + 10^{\left(0.09018 + \frac{2729.92}{T} - \text{pH}\right)}} \quad (4)$$

FAN is the free ammonia nitrogen concentration (mg NH₃-NL⁻¹), TAN is the total ammoniacal nitrogen concentration (mg NL⁻¹), and *T* is the temperature (K).

2.4 | Analytical Methods

Online measurements and controls in the digester system include temperature; masses of sludge and digestate; overpressure in the digester (PTX1400, GE Druck); levels of CH₄, CO₂, H₂S, and O₂ in the biogas (gas analyser BIOLYZER, AFRISO); and

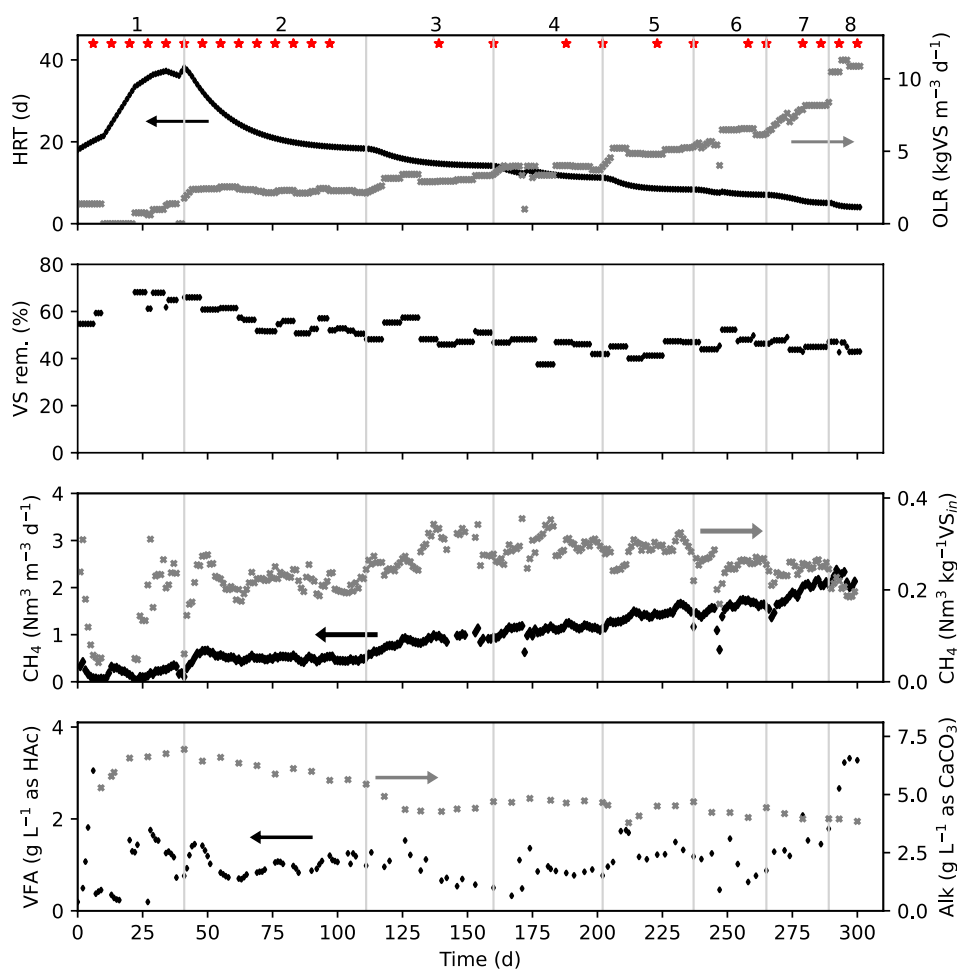


FIGURE 1 | Hydraulic retention time (HRT), organic loading rate (OLR), removal efficiency of volatile solids (VS), specific CH_4 production normalised to the reactor volume or the VS loaded to the reactor, volatile fatty acid (VFA) and total alkalinity (Alk) concentrations in the reactor over time. Sampling points for DNA are marked with red asterisks (*) in the upper panel. Vertical lines show major changes in OLR. Numbers on top show phases of the experiment (see Table 1). As indicated by the black and grey arrows, data series shown with black points correspond the left y-axis while data series shown with grey crosses correspond the right y-axis in the panels.

biogas flow (flow meter, model GD6471, Fluid Inventor AB). Other analytical methods such as volatile fatty acids (VFA), alkalinity, and ammonium (i.e., TAN), TS, VS, foam, and pH measurements were carried out as specified in Data S1.

2.5 | DNA Extraction and Sequencing

Sludge samples were collected from the reactor on 26 occasions (Figure 1). The samples were kept frozen at -20°C until DNA extraction, which was done using the FastDNA Spin Kit for Soil (MP Biomedicals). The manufacturer's protocol was followed except for an extra homogenization step as described in Abadikhah et al. (2022). DNA sequencing was carried out by Eurofins Genomics, where library preparation was done using a protocol based on the *NEBNext Ultra II FS DNA Library Prep Kit for Illumina*, and paired-end 2×150 base pair (bp) sequencing was done on the NovaSeq 6000 platform. The raw sequence reads are deposited at the NCBI SRA with bio-project [PRJNA973019](https://www.ncbi.nlm.nih.gov/bioproject/PRJNA973019).

2.6 | Bioinformatics

Initial read-based analysis of microbial community composition was done using SingleM and MetaPhlan4 (Blanco-Míguez et al. 2023; Woodcroft et al. 2024). The SingleM output was grouped at the genus level, pairwise dissimilarities between samples were calculated using a Hill-based index with diversity order 1 (Modin et al. 2020), and a principal coordinate analysis (PCoA) was carried out to visualise the differences in community composition between samples. Another PCoA using the MetaPhlan4 output showed a similar pattern (Figure S2). Based on the PCoAs, the samples were divided into four groups. Assembly and binning of contigs were done for each group of samples using the following steps: (1) Quality-filtering was done using fastp v0.20.0 (Chen et al. 2018); (2) normalisation to a target depth of 100 and mindepth of 2 was done using BBNorm (BBMap v38.61b, sourceforge.net/projects/bbmap); (3) assembly was done using Megahit v1.2.9 with presets meta-large (Li et al. 2015); (4) reads from each sample were mapped to the contigs using Bowtie v2.3.5.1

(Langmead and Salzberg 2012) and Samtools v1.10 (Danecek et al. 2021), binning was done using Metabat v2.12.1 (Kang et al. 2019), BinSanity v0.5.4 (Graham et al. 2017), and Vamb v3.0.2 (Nissen et al. 2021); and (5) consensus bins were determined using DASTool v1.1.4 (Sieber et al. 2018). The bins from all four groups of samples were combined and dereplicated using dRep v3.3.0 (Olm et al. 2017) with an average nucleotide identities (ANI) threshold of 0.95. The dereplicated bins can be considered species representatives (Olm et al. 2020). To further refine the bins, the completeness and redundancy were checked with Anvio v7 (Eren et al. 2021). Bins with high completeness (> 90%) but also high redundancy (> 5%) were manually refined using anvirefine. Bins with low completeness (< 90%) but low redundancy (< 5%) were reassembled with sequence reads from all 26 samples using the reassemble_bins module in MetaWrap (Uritskiy et al. 2018). Finally, the completeness and redundancy (contamination) of all the bins were checked with both CheckM (Parks et al. 2015) and Anvio. Bins that had a completeness > 50% and redundancy < 10% with one of the methods were retained for further analysis. Taxonomic affiliations of the bins were determined using GTDB-TK with database R207 (Chaumeil et al. 2022).

The relative abundances of the bins were determined using CoverM v0.6.1 (github.com/wwood/CoverM) with bwa-mem as mapping software (Vasimuddin et al. 2019). The relative abundance of a bin in a sample was set to 0 if less than 50% of the nucleotides in the bin were covered by at least one read.

The coding sequences (CDS) of the bins were predicted and annotated using Prokka v1.14.6 (Seemann 2014), which uses Prodigal (v2.6.3) to determine amino acid sequences of the translated CDS. Functional annotation was also performed by Interproscan v5.64–92.0 and by querying the translated CDS amino acid sequences against reference sequences using BLASTP implemented in DIAMOND (Buchfink et al. 2021). Criteria for categorising taxa as putative acetogens, syntrophic acetate-oxidising bacteria (SAOB), syntrophic propionate-oxidising bacteria (SPOB), sulfate-reducing bacteria (SRB), and methanogens, as well as the gene annotations and database accession codes used to identify genes involved in methanogenesis, Wood-Ljungdahl, glycine cleavage, methylmalonyl-CoA, and dissimilatory sulfate reduction pathways are listed in Data S2. For identification of genes encoding enzymes responsible for hydrolysis of polysaccharides, lipids, and polypeptides, the CAZ (Drula et al. 2021), lipase engineering v4.1.0 (Fischer and Pleiss 2003), and MEROPS (Rawlings et al. 2017) databases were used. For the CAZ database, CAZy-Parser (Honorato 2016) was used to download sequences of glycoside hydrolases, polysaccharide lyases, and carbohydrate esterases. For the MEROPS database, peptidase inhibitors were removed manually.

Phylogenetic trees were constructed using PhyloPhlan v3.0.67 (Asnicar et al. 2020). Reference genome assemblies were downloaded from NCBI (ncbi.nlm.nih.gov/sites/batchentrez). The phylogenetic trees were rooted with *Methanopyrus kandleri* (GCA_000007185.1) as the outgroup and plotted using ete3 (Huerta-Cepas et al. 2016) or pyCirclize ([\[pyCirclize\]\(https://github.com/moshi4/pyCirclize\)\). FastANI v1.33 \(Jain et al. 2018\) was used to calculate average nucleotide identities \(ANI\).](https://github.com/moshi4/</p>
</div>
<div data-bbox=)

2.7 | Statistical Methods

Correlations in occurrence between bins were estimated using FastSpar (Watts et al. 2018), which is based on the SparCC algorithm (Friedman and Alm 2012) and Spearman's ρ calculated using Scipy (Virtanen et al. 2020). The network was constructed and analyzed using NetworkX (Hagberg et al. 2008) and was based on significant pairwise correlations ($p < 0.05$) with a correlation coefficient > 0.5 with both FastSpar and Spearman.

The weighted average fraction of hydrolysis genes in a sample was calculated using Equation (5).

$$g_s = \sum_{i=1}^N \left(g_i \cdot \frac{p_{i,s}}{\sum_{i=1}^N p_{i,s}} \right) \quad (5)$$

where g_s is the weighted average fraction of genes in sample s ; g_i is the fraction of genes in species i ; $p_{i,s}$ is the relative abundance of species i in sample s ; and N is the total number of bins.

3 | Results

3.1 | Reactor Performance

During the temperature transition in phase 1, the volumetric CH_4 production rapidly dropped from $0.42 \text{ Nm}^3 \text{ m}^{-3} \text{ d}^{-1}$ on Day 2 to $0.06 \text{ Nm}^3 \text{ m}^{-3} \text{ d}^{-1}$ on Day 8. Due to equipment malfunction, the OLR was zero between Day 10 and 21. Once the substrate feeding was resumed, the CH_4 production gradually increased from 0.03 to a relatively stable production rate of $0.51 \pm 0.6 \text{ Nm}^3 \text{ m}^{-3} \text{ d}^{-1}$ in Phase 2. During Phases 3–8, the volumetric CH_4 production increased with increasing OLR. The specific CH_4 production rate, normalized to the mass of VS fed to the reactor, peaked at $0.31 \pm 0.06 \text{ Nm}^3 \text{ kg}^{-1} \text{ VS}_{\text{in}}$ in phase 4 when the OLR was $3.5 \pm 0.9 \text{ kgVS m}^{-3} \text{ d}^{-1}$ and the HRT approached 11.3 d. In phases 7–8, the specific CH_4 production rate dropped to $0.23 \pm 0.02 \text{ Nm}^3 \text{ kg}^{-1} \text{ VS}_{\text{in}}$ when the OLR and HRT approached $11.3 \text{ kgVS m}^{-3} \text{ d}^{-1}$ and 4.0 d, respectively (Figure 1). Previous studies of thermophilic anaerobic digestion of sewage sludge have found optimal specific methane production at an OLR of around $2.5\text{--}3.7 \text{ kgVS m}^{-3} \text{ d}^{-1}$ and deteriorating performance above $7.5 \text{ kgVS m}^{-3} \text{ d}^{-1}$ (Braguglia et al. 2015; Liu et al. 2017).

The VS removal peaked at 68% in phase 1 when the HRT was high and the OLR was low. During Phase 2, it approached 50%, and the mean values for the following phases with increasing OLR were in the range 44%–48%. The total VFA concentration was high in the initial samples following reactor startup, reaching

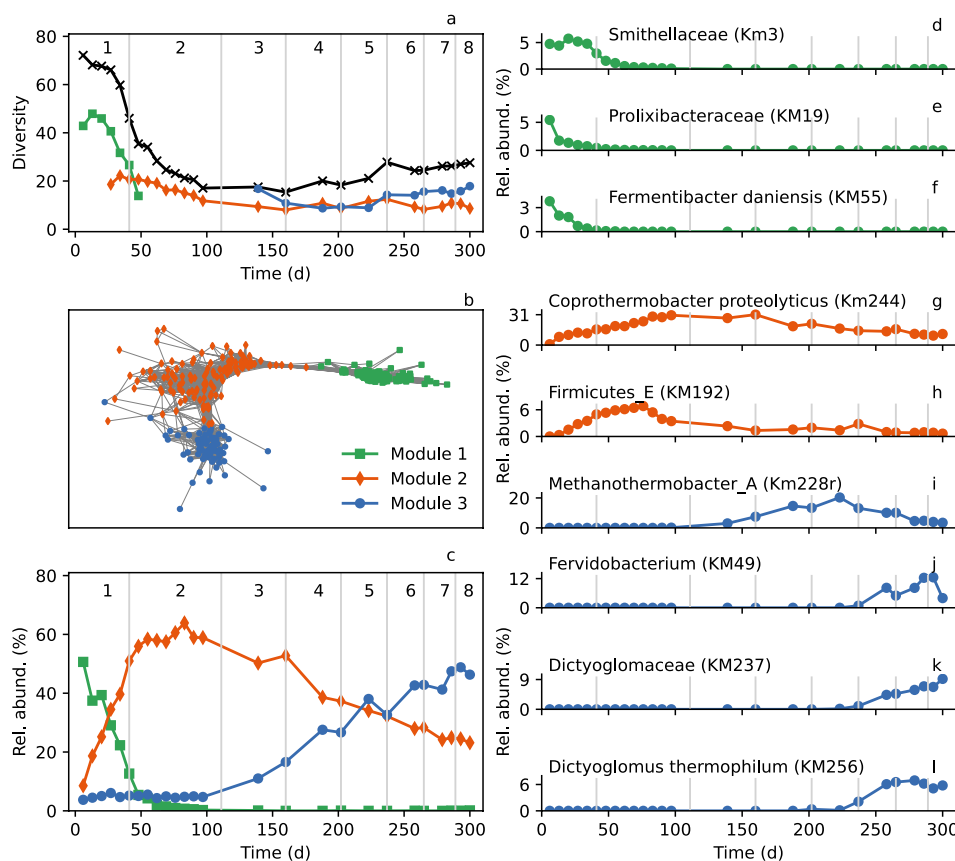


FIGURE 2 | (a) Diversity (1D) of the microbial community (black line), and the diversity of species in each network module. (b) Network showing positive correlations (edges) between species (nodes). The major modules of clustered species are indicated in the legend. (c) The total relative abundance of all species in each major module over time. (d–l) The relative abundance of the most abundant species in the experiment. Time periods marked with grey lines show the eight experimental phases.

3.1 gHAc L⁻¹ on Day 6. Then, the VFA concentration was stable until the final phases, when it increased from 1.5 ± 0.3 gHAc L⁻¹ in Phase 7 to 3.1 ± 0.3 gHAc L⁻¹ in Phase 8. However, the alkalinity was sufficiently high to maintain a stable pH of 7.0–7.3 throughout the experiment (Figure 1, Figure S3). Acetate was the dominating VFA, with concentrations typically around 1.0 g/L, except in Phases 1 and 8, where concentrations exceeding 3.0 g L⁻¹ could be observed. Propionate and iso-valerate were detected in concentrations up to 1.1 g L⁻¹ and 0.4 g L⁻¹ in phases 1 and 8, respectively. The TAN concentration decreased from 1.8 g N L⁻¹ in Phases 1 to 1.0–1.2 g N L⁻¹ in Phases 3–8, indicating decreasing efficiency of protein degradation with increasing OLR. Similarly, the free ammonia concentration decreased from a peak of 0.2 g N L⁻¹ to 0.04–0.07 g N L⁻¹ in Phase 1 and Phases 3–8, respectively. In contrast, the H₂S proportion in the produced gas increased gradually from Phase 4 and with increasing OLR. Some high values could also be observed in Phase 1. H₂S is produced during the degradation of sulfur-containing proteins and via the activity of sulphate-reducing bacteria (Daly and Ni 2023). Foam was observed in the reactor at the end of Phase 4 and remained until the end of the experiment (Figure S3). The H₂S levels and foaming problems at the end of the experiment increased with increasing OLR. Overload and fluctuations in OLR are reported as the most common causes of foaming in full-scale anaerobic digesters because of the accumulation of organic compounds such as surface-active substances (Yang et al. 2021).

3.2 | Microbial Community Structure

3.2.1 | Diversity Decreased During Adaptation to Thermophilic Conditions

Sequencing of the 26 samples collected at the time points shown in Figure 1 resulted in the assembly of 304 species-level genome bins (SGB), which represented 61%–74% of the sequence reads. Among the SGB, 109 could be classified as high-quality draft metagenome-assembled genomes (MAGs) with >90% completion and <5% redundancy according to both CheckM and Anvio; 182 were medium-quality draft MAGs with >50% completion and <10% redundancy (according to reporting standards suggested in Bowers et al. 2017); and 13 were low quality with either a completeness <50% or a redundancy >10% in one of the quality control methods. Detailed information about the SGB, including size, number of contigs, N50, completeness, redundancy, and taxonomic affiliation, is shown in Data S1.

The species diversity in the reactor was calculated as the Hill number with order 1 (1D) (Jost 2006). This diversity index takes relative abundance into account and can be interpreted as the number of species that are common in a community. For the whole community, the diversity dropped from 72 in the beginning of the experiment to 15 in phase 3. Then it gradually increased again, eventually reaching 28 (Figure 2a). The assembly- and binning-independent methods SingleM and Metaphlan4

showed the same alpha- and beta diversity patterns as the analysis with assembled SGB.

3.2.2 | Network Analysis Revealed a Microbial Community Succession

All 304 SGB were included in a network analysis, which revealed three major modules (Figure 2b). Each module can be considered a subcommunity of co-occurring taxa. Module 1 included 99 SGB, which made up 50% of the community at the first sampling point but rapidly decreased in relative abundance to less than 1% by Day 76. Module 2 included 118 SGB, which rapidly increased in relative abundance from 8% on Day 6 to 62% on Day 83 (phase 2). The SGB in this module then gradually decreased down to a relative abundance of 22% at the end of the experiment. Module 3 included 68 SGB, which made up less than 6% of the community until Day 139 (Phase 3). Then, they gradually increased in relative abundance, reaching 47% at the end of the experiment. There were 19 SGB that could not be placed in a network module. They represented a minor part of the community, having a relative abundance of 2% at the first sampling point and then ranging between 0.3% and 1.1% at the other sampling points. The network analysis, thus, showed a succession between three major subcommunities during the experiment (Figure 2c).

3.2.3 | Microbial Community Composition of the Network Modules

The microbial community composition of the three networks modules is shown in Figure S4. Module 1 contained mesophilic taxa that were inactivated and gradually washed out from the reactor during the thermophilic acclimatisation in Phases 1–2. It had high diversity (Figure 2a) and several phyla, including *Cloacimonadota*, *Desulfobacterota*, *Fermentibacterota*, *Spirochaetota*, and *Verrucomicrobiota*, were exclusively found in Module 1 (Figure S4) and have previously been observed in mesophilic anaerobic digesters (Kirkegaard et al. 2016; Vanwonterghem et al. 2016; Dyksma and Gallert 2022; Wang, Chen, and Chang 2024; Wang, Zhang, et al. 2024). Modules 2–3 contained thermophilic taxa and had lower diversity than module 1 (Figure 2a). Among bacteria, Modules 2–3 had larger numbers of SGB within *Actinobacteriota*, *Proteobacteria*, and *Firmicutes* in comparison to Module 1. The diversity of archaea was high in module 1, with seven detected SGB from three phyla (*Halobacteriota*, *Methanobacteriota*, *Thermoproteota*). Modules 2 had three archaeal SGB in *Halobacteriota* and *Methanobacteriota*, while module 3 only had one in *Methanobacteriota* (Figure S4).

The nine most abundant SGB in the three modules are shown in Figure 2d–f. Only three could be taxonomically classified at the species level. *Candidatus Fermentibacter daniensis* (KM55) in Module 1 is known to be abundant in mesophilic anaerobic digesters at wastewater treatment plants and likely contributes to the fermentation of sugars into acetate and hydrogen (Kirkegaard et al. 2016). *Coprothermobacter proteolyticus* (Km244) in Module 2 reached a relative abundance of 30% in Phase 3. This is a known thermophilic species that has been

observed in other thermophilic anaerobic digesters treating sewage sludge (Wu, Shan, et al. 2020; Wu, Lin, et al. 2020). The species degrades peptides and some sugars, while producing acetate, H₂, and CO₂ as main products (Olliver et al. 1985). *Dictyoglomota thermophilum* (KM256), another *Dictyoglomataceae* sp. (KM237), and a *Fervidobacterium* sp. (KM49) increased rapidly in relative abundance at the end of the experiment. The phylum *Dictyoglomota* contains members that are extremely thermophilic, and the type strain *D. thermophilum* is saccharolytic and ferments various carbohydrates to mainly acetate, lactate, H₂, and CO₂ (Patel et al. 1987). The most abundant SGB also included a *Smithellaceae* sp. (Km3) and a *Prolixibacteraceae* sp. (KM19) in Module 1, a *Firmicutes* E sp. (KM192) in Module 2, and a *Methanothermobacter* sp. (Km228r) in Module 3. The latter in Module 3 reached a relative abundance of 20% in phase 5.

3.3 | Functional Analysis of Species-Representative Genome Bins (SGB)

Using gene annotation and phylogenetic analysis, taxa putatively involved in hydrolysis and fermentation, syntrophic propionate oxidation, acetogenesis, syntrophic acetate oxidation, sulfate reduction, and methanogenesis were identified (Figure 3).

3.3.1 | Hydrolysis and Fermentation

Microorganisms involved in the hydrolysis of polysaccharides, lipids, and polypeptides were identified by genes annotated as encoding CAZymes, lipases, and peptidases, respectively. All SGB except four *Methanobacteriota* spp. contained hydrolysis genes. The fraction of hydrolysis genes in each SGB was calculated, and for each sample, the weighted average fraction of hydrolysis genes was determined (Figure 3a). The fraction of CAZyme genes initially dropped from 1.4% on Day 6 to 0.7% in Phase 3–5 but increased again to 1.6% in Phase 8. The fraction of lipases peaked at 4.6% in phase 1, dropped to 3.8%–4.0% in Phase 3–5, and then increased to 4.6% again in Phase 8. The fraction of peptidases increased from 2.7% on Day 6 to 3.3% in phase 2, after which it gradually decreased to 2.9% in phase 8. Previous research has shown that the composition of hydrolysis genes in the microbiome changes as a result of changes in the feed composition (Orellana et al. 2022). Here, it appears to change both by the temperature change and by the increase in OLR during thermophilic conditions.

In module 1, major hydrolytic and fermentative taxa included a *Smithellaceae* sp. (Km3) and an *Anaerolineae* (KM72), which both had a high fraction of lipase genes, as well as a *Prolixibacteraceae* sp. (KM19), which had the highest fraction of CAZyme genes among the SGB (Figure S5). The family *Smithellaceae* contains several species known to degrade short-chained fatty acids (Galushko and Kuever 2021). In Module 2, the dominant *Coprothermobacter proteolytica* (Km244, Figure 2g) had a low fraction of CAZyme genes but was among the top 3% of SGB in terms of peptidase gene content. This taxon is known to be proteolytic and has been identified in several studies of the microbial community structure in anaerobic thermophilic reactors (Gagliano et al. 2015). Other abundant taxa in Module 2 included a *Firmicutes* E sp. (KM192), which was among the top 1%

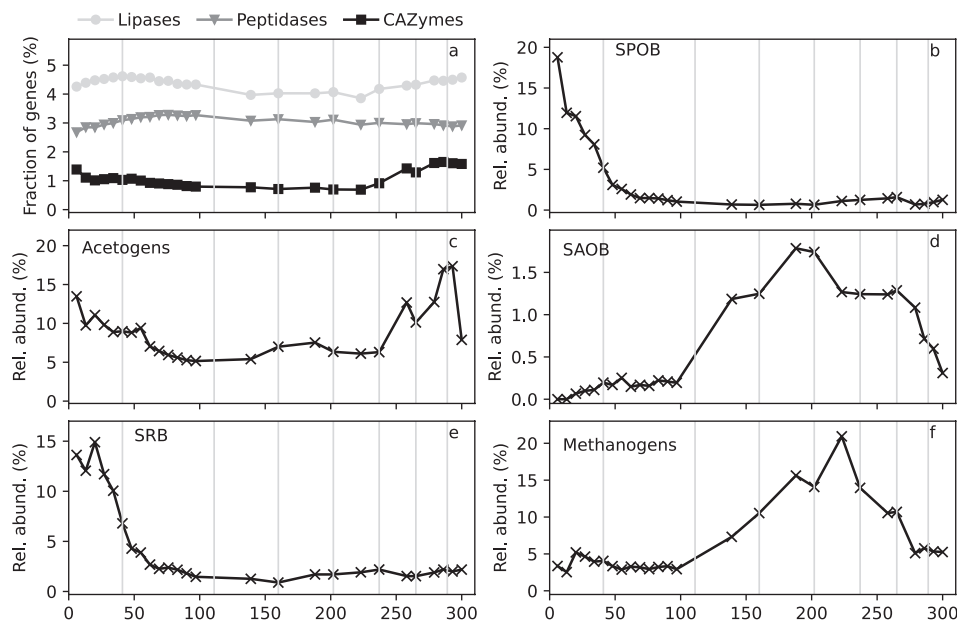


FIGURE 3 | (a) Weighted average fraction of lipase-, peptidase-, and CAZyme genes per SGB. (b-f) Relative abundances of putative syntrophic propionate oxidising bacteria (SPOB) (b), acetogens (c), syntrophic acetate oxidising bacteria (SAOB) (d), sulfate-reducing bacteria (SRB) (e), and methanogens (f). Time periods marked with grey lines show the eight experimental phases. The criteria for including SGB within the functional groups are listed in Data S2.

in terms of peptidase content, and a *Limnochordia* sp. (KM261), which had quite a high gene fraction in all three groups of hydrolysis genes. *Microthrix parvicella* (KM249) and another *Microthrix* sp. (Km109) were also abundant in Modules 2 and 3, respectively. Both species had a high fraction of lipase genes. In Module 3, a *Fervidobacterium* sp. (KM49) belonged to the top quartile of SGB in terms of CAZyme content. *Fervidobacter* is a well-known hydrolytic taxon (Javier-López et al. 2024). *Dictyoglomota thermophilum* (KM256) and the *Dictyoglomaceae* sp. (KM237) belonged to the top quartile in terms of lipases and peptidases and the top 10% in terms of CAZymes (Figure S5), which is consistent with *D. thermophilum* being known as a saccharolytic thermophile (Patel et al. 1987).

3.3.2 | Syntrophic Propionate Oxidation

Propionate is an intermediate in the fermentation process, and its accumulation can indicate process failure. Thermophilic anaerobic digesters suffer from high propionate concentration more often than mesophilic digesters (Wiegant et al. 1986). The presence of SPOB was analysed by taxonomic affiliation to families or genera known to contain SPOB and by the presence of genes for all steps of the methylmalonyl-CoA (mmc) pathway (Westerholm et al. 2021). The relative abundance of putative SPOB decreased rapidly in phase 1 (Figure 3b). Module 1 had 15 SGB classified as putative SPOB (Figures S6–S10). These included three *Smithellaceae* spp. and four Syntrophosphaera spp., which are known to harbour SPOB (Liu et al. 1999; Dykma and Gallert 2019) and are affiliated with mesophilic conditions (Chen et al. 2020). The dominating *Smithellaceae* sp. (Km3, Figure 2d) was also classified as a hydrolytic bacterium because of its high proportion of lipases and peptidases. *Ca.* Syntrophosphaera thermopropionivorans (Km269) also had high relative abundance in the mesophilic sludge but was eliminated from the reactor

during the temperature increase in Phase 1 (Figure S10d). The species was previously identified in a thermophilic propionate oxidising reactor, but other Syntrophosphaera spp. have been associated with mesophilic conditions (Dykma and Gallert 2019). The genus *Smithella*, as well as representatives of Cloacimonadaceae, e.g., Syntrophosphaera, are commonly detected potential propionate degraders in sludge-based processes (Puengrang et al. 2020; Johnson and Hug 2022).

In Module 2, none of the most abundant putative SPOB was identified at the species level (Figure S10g–j). The most abundant taxon was a bacterium (KM79) with the placeholder species name DTU030 sp012842325 in GTDB. It belongs to the family *Smithellaceae* and has previously been assembled from anaerobic digesters (Campanaro et al. 2020). KM108 was classified as a *Pelotomaculaceae* spp., which is a family known to contain SPOB that thrive under thermophilic conditions (Imachi et al. 2002) and also at elevated ammonia levels, i.e., $1.2 \text{ g NH}_3 \text{ L}^{-1}$ (Singh et al. 2023). In Module 3, a SGB classified as *Thermanaerotherix daxensis* (Km304) within the class *Anaerolineae* was most abundant, reaching a relative abundance of 0.7% in Phase 6. The species is known as a thermophilic anaerobe that ferments sugars (Grégoire et al. 2011). However, other *Anaerolineae* species have been isolated from propionate-degrading thermophilic environments, although they have not been identified as propionate oxidizers (Yamada et al. 2007). A *Kapabacteriales* sp. (KM58), which had UBA2268 as a family-level placeholder in GTDB but was unclassified at the genus level, reached 0.3% and appeared in the reactor during the period with the highest specific methane production rate and co-occurred with the dominating methanogen (Km228r) (Figure S10l). This SGB also had all genes in the methylmalonyl-CoA pathway, including a gene annotated as propionate CoA-transferase, which was lacking in many of the other putative SPOB (Figure S9). To our knowledge, this is the first report on a potential propionate oxidiser in this order.

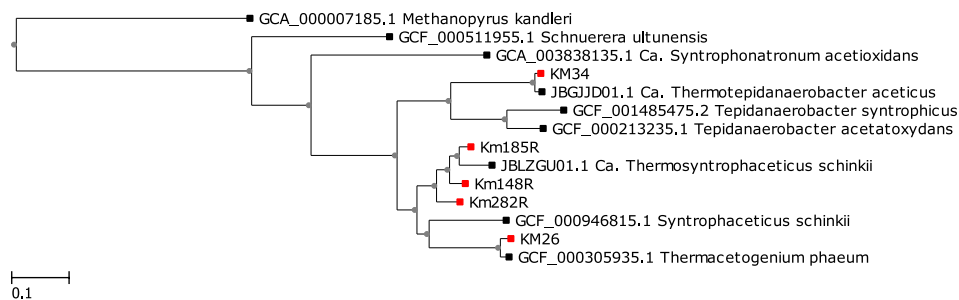


FIGURE 4 | Phylogenetic tree of five SGB related to known SAOB. *Methanopyrus kandleri* was used as an outgroup.

However, this species belongs to phylum *Bacteroidota*, known to harbour many propionate producers, and thus its role in the present reactors cannot be concluded (Döring and Basen 2024).

3.3.3 | Acetogenesis and Syntrophic Acetate Oxidation

Previous research has shown that acetate conversion in thermophilic anaerobic digestion can be carried out via syntrophic acetate oxidation coupled to hydrogenotrophic methanogenesis instead of acetoclastic methanogenesis (Ahring 1995). The reverse process, homoacetogenesis, is not a dominating process in well-functioning digesters but could occur at low temperature and low or high pH (Pan et al. 2021). Several studies have hypothesized that SAOB use the Wood-Ljungdahl pathway, in some cases coupled with the glycine cleavage pathway (Li et al. 2022; Puchol-Royo et al. 2023; Zeng et al. 2024). However, based on this pathway analysis it is difficult to completely clarify if the retrieved candidates are acetate oxidisers or acetate producers as both SAOB and known acetogens have been shown to use Wood-Ljungdahl alone or in combination with the glycine cleavage pathway (Manzoor et al. 2018; Keller et al. 2019; Song et al. 2020).

Gene annotations identified 23, 25, and 15 SGB with genes from the Wood-Ljungdahl alone or in combination with the glycine cleavage pathway in Modules 1, 2, and 3, respectively (Figures S11–S14). The total relative abundance of these taxa was highest in Phases 1 and 7–8 (Figure 3c). In Modules 1–2, the most abundant taxa were all unclassified or had placeholder names at the genus level (Figure S15). Few SGB had a complete Wood-Ljungdahl pathway and the key enzyme CODH was missing for most SGBs, suggesting they were not true homoacetogens. The most dominant taxa in Modules 1, 2, and 3 instead included several taxa identified to have hydrolytic/fermentative abilities such as *Anaerolineae*, *Fervidobacterium* sp. (KM49, Figure 2j), and *Acetomicrobium flavidum* (KM27) (Soutschek et al. 1984; Andrews and Patel 1996; Xia et al. 2016).

Five SGB were identified as putative SAOB based on phylogenetic relatedness to known SAOB and the presence of key genes in the Wood-Ljungdahl and glycine cleavage pathways (Figure 4, Figure S16). The putative SAOB peaked in relative abundance in Phase 4 (Figure 3d). The most abundant, KM26, was classified as *Thermacetogenium phaeum* (>96% ANI), a known SAOB (Hattori et al. 2000). KM34 was nearly identical to *Ca. Thermotepidanaerobacter aceticus* (>99% ANI), a potential SAOB recently discovered in reactors operated with

household- and food waste with a high ammonia concentration (0.7–1.0 gN/L) and thermophilic conditions (Cheng et al. 2025). As the ammonia concentration in our study was relatively low (Figure S3), it suggests that temperature rather than ammonia drives the selection of *Ca. Thermotepidanaerobacter aceticus* in the reactor. Km148R, Km185R, Km282R formed a clade with *Ca. Thermosyntrophaceticus schinkii* (Figure 4), another potential SAOB recovered by Cheng et al. (2025). The ANI values were 88%–91%, suggesting that the four taxa in the clade were different species.

3.3.4 | Hydrogen Sulfide Production

SRB are known to compete with methanogens for substrates, and the produced hydrogen sulfide contaminates the biogas (Visser et al. 1996). Putative SRB were identified by searching for genes annotated as sulfate adenylyltransferase (*sat*), adenylylsulfate reductase (*apr*), and dissimilatory sulfite reductase (*dsr*, *asr*, or *sirA*) (Figures S17–S20). Metabolic potential for sulfate and sulfite reduction is known to be widespread among bacteria and archaea (Anantharaman et al. 2018), and in total, 25 SGB could be classified as putative SRB. Most of these had partial pathways, typically lacking either *sat* or the subunit *aprA*. Module 1 had 17 putative SRB. These included four *Desulfurobacterota* spp., including the highly abundant *Smithellaceae* sp. (KM3) (Figure S18). *Desulfurobacterota*, formerly part of *Deltaproteobacteria* (Waite et al. 2020), is a phylum known to contain SRB (Anantharaman et al. 2018). Modules 2 and 3 had four and six putative SRB, respectively. A *Pelotomaculaceae* sp. (KM108, also a putative SPOB) and a *Burkholderiaceae* sp. (KM246R) in Module 2, and a *Firmicutes* G sp. (KM276) and a *Casimicrobiaceae* sp. (KM200) in Module 3, all had nearly complete pathways and possessed *sat*, *aprAB*, and multiple *asr* or *dsr* subunits (Figures S19, S20). Species within *Firmicutes* as well as *Pelotomaculum* spp. have previously been suggested to be capable of sulfate reduction (Dong et al. 2016), but *Burkholderiaceae* and *Casimicrobiaceae* have not. The most abundant taxa were *Acidovorax defluvii* (KM136) and Km246R in Module 2, both reaching over 0.5% relative abundance, and *Defluviitoga tunisiensis* (KM151) and a *Syntrophomonadaceae* sp. (KM277) in Module 3, both reaching a relative abundance of about 1% (Figure S21). *Acidovorax defluvii* has been associated with sulfur metabolism in sewer biofilms (Satoh et al. 2009) and has also been detected under thermophilic conditions (Cheng et al. 2013). *Defluviitoga tunisiensis* was previously shown to reduce thiosulfate and elemental sulfur, but not sulfite or sulfate (Ben Hania et al. 2012). The total relative abundance of putative

SRB was lowest in Phase 3, which coincided with the lowest H₂S content in the biogas (Figure 3e, Figure S3).

3.3.5 | Methanogenesis

All 11 archaeal SGB in the dataset were methanogens. The total relative abundance of methanogens was lowest during Phase 1 (Figure 3f), but the diversity was the highest. Six out of the seven belonging to Module 1 had the highest relative abundance in the initial samples and then rapidly decreased and disappeared from the reactor. These mesophilic methanogens included hydrogenotrophic (e.g., *Methanoregulaceae*, Km218r), acetoclastic (*Methanotrix*, KM25), and methylotrophic (*Ca. Methanomethylicus*, KM95) taxa (Figures S22, S23). An SGB classified as *Methanothermobacter marburgensis* (Km197) was absent in the initial samples, then peaked at a relative abundance of 0.16% on Day 27, and disappeared from the reactor from Day 69 (Figure S24). This thermophilic and hydrogenotrophic methanogen (Fuchs et al. 1978) was outcompeted by two other *Methanothermobacter* spp. (*M. thermautotrophicus*, KM279, and *M. wolfeii*, KM64R) in Module 2, which were abundant during Phases 1–4. Module 2 also included *Methanosarcina thermophila* (KM84), which possessed a full set of genes for hydrogenotrophic, acetoclastic, and methylotrophic methanogenesis. The species is metabolically versatile but prefers to use the acetoclastic pathway (Lackner et al. 2018). Only one SGB belonged to Module 3. This *Methanothermobacter* (Km228r), unclassified at the species level, peaked at a relative abundance of 15%–20% in Phases 4–5 but decreased to 3% at the end of the experiment. It only possessed the metabolic pathway for hydrogenotrophic methanogenesis.

4 | Discussion

Three major stages in reactor function could be observed: the stabilisation stage, the peak performance stage, and the deterioration stage. The stabilisation stage occurred in Phases 1–2 when stable biogas production was reached after the temperature increase and initial instability. The peak performance stage occurred in Phase 4 when the specific methane production was the highest. The deterioration stage occurred in Phases 7–8 when the specific methane production dropped and foaming, H₂S content in the biogas, and propionate concentration in the liquid increased. Different SGB were associated with the three stages.

4.1 | Stabilisation Stage

During the initial acclimatisation phase, taxa associated with mesophilic conditions rapidly disappeared from the reactor. After 48 days, the total relative abundance of the 99 SGB in Module 1 had decreased from over 50% to about 5% (Figure 2c). Some taxa, such as the second most abundant methanogen in Module 1, a *Methanoculleus* sp. (KM265), completely disappeared from the reactor after only 27 days (Figure S24). This rapid change in community composition was associated with signs of instability in reactor performance. Accumulations of propionate in the liquid and a peak of H₂S in the biogas during

Phase 1 suggest less efficient hydrogen removal and increased activity of SRB. Hydrogen removal is critical for the activity of SPOB, and the decreased abundance of hydrogenotrophic methanogens likely caused propionate to accumulate. Methanogens and sulfate reducers compete for the same substrates, and, in addition, SRB can also utilise propionate (Stefanie et al. 1994). Thus, the decrease in abundance of hydrogenotrophic methanogen and increased levels of hydrogen and propionate might have enhanced the growth of SRB. However, even though H₂S production is not known to be particularly associated with thermophilic conditions (Vu et al. 2022), its solubility in liquid decreases with increasing temperature and decreasing pH. Thus, high H₂S content in Phase 1 could also partly have been associated with the change in operational conditions.

In Phase 2, the reactor had stabilised, and the biogas production had recovered. The diverse community of hydrolytic and fermentative mesophilic bacteria in Module 1 had been replaced by a less diverse community dominated by *Coprothermobacter proteolyticus* (Km244) (Figure 2). The observed lower diversity and evenness at thermophilic conditions compared to the mesophilic sludge used to inoculate the reactor is in line with several previous studies of anaerobic digestion (De Vrieze et al. 2015; Westerholm et al. 2017; Steiniger et al. 2023). Among SPOB, the diverse community of *Smithellaceae* spp. and *Syntrophosphaera* spp. had been replaced by a *Pelotomaculaceae* sp. (KM108) and other putative SPOB (Figures S8, S10). This result was in line with a previous study showing a diverse mesophilic SPOB community consisting of *Syntrophobacter*, *Smithella*, and *Syntrophomonas* and a thermophilic SPOB community dominated by *Pelotomaculum* in lab reactors operated with propionate as the sole carbon source (Chen et al. 2020). The mesophilic methanogens dominated by acetoclastic species were replaced by three *Methanothermobacter* spp. (*M. marburgensis*, Km197; *M. autotrophicus*, KM279; and *M. wolfeii*, KM64R) and *Methanosarcina thermophila* (KM84) (Figure S24). They likely produced methane and acted as sinks for both H₂ and acetate during the stabilisation stage. The emergence of a *Tepidanaerobacteraceae* sp. (KM34), closely related to a known SAOB (Figure 4), suggested that syntrophic acetate oxidation had started to play a role for methane production in the reactor.

4.2 | Peak Performance Stage

The peak reactor performance in terms of specific biogas production occurred in Phase 4 with an OLR of $3.5 \pm 0.9 \text{ kgVS m}^{-3} \text{ d}^{-1}$ and an HRT approaching 11.3 d. *Coprothermobacter proteolyticus* (Km244) was still the dominating hydrolytic taxon. Among putative SPOB, the *Pelotomaculaceae* sp. (KM108) was still present and had been accompanied by a *Kapabacteriales* sp. (KM58) (Figure S10). The largest shift had occurred for methanogens, which were dominated by a new *Methanothermobacter* sp. (Km228r). It first appeared in the reactor in Phase 3 and reached a relative abundance of 10%–20% between Day 188 and Day 265 (Figure 2i). The rise of Km228r coincided with the appearance of *Thermacetogenium phaeum* (KM26), a known SAOB, which peaked with a relative abundance of 1.7% in Phase 4 (Figure S16). KM26 and Km228r co-occurred in the reactor and were directly connected to each other in the network analysis. This suggests a transition from the stabilisation phase, where *Methanosarcina*

thermophila (KM84) likely produced methane via acetoclastic methanogenesis alongside syntrophic acetate oxidation involving KM34 and three *Methanothermobacter* species, to the peak performance stage, where acetate mainly was consumed via syntrophic acetate oxidation by KM26 and three other putative SAOB within the *Thermoacetogeniaceae* family, in association with Km228r acting as the sole methanogen (Figure S16).

4.3 | Deterioration Stage

The gradual increase in OLR eventually led to process deterioration with foaming and H₂S content in the biogas gradually increasing from Phases 4 to 8, and increased VFA concentration and reduced pH in Phase 8 (Figure 1, Figure S3). *Microthrix parvicella* (KM249) and another *Microthrix* sp. (Km109) were present in the reactor with the combined relative abundance increasing from 2.1% on Day 139 to 7.5% on Day 300 (Figure S5). This coincided with a gradually increasing foaming index (Figure S3). *Microthrix parvicella* is known as a filamentous bacterium commonly associated with bulking and foaming of activated sludge systems (Rossetti et al. 2005), but they have also been shown to grow in mesophilic anaerobic digesters (Ganidi et al. 2011; Lienen et al. 2014). Here, they appear to grow also under thermophilic conditions and may contribute to foaming. The gradual increase in H₂S content in the biogas was associated with a gradual decrease in the relative abundance of the dominating methanogen (Km228r) from peaking at 20% on Day 223 to 3.4% on Day 300. This may have opened up opportunities for SRB to compete with the hydrogenotrophic methanogen for the available H₂. For example, *DeFluviitoga tunisiensis* (KM151), previously shown to produce hydrogen sulfide from sulfur and thiosulfate (Ben Hania et al. 2012), and a *Moorellia* sp. (KM257) classified as a putative SRB, increased in relative abundance (Figure S21). Furthermore, a decrease in the relative abundance of *Thermacetogenium phaeum* (KM26) and other putative SAOB made more acetate available for SRB. The acetate was likely also exploited by *Methanosarcina thermophila* (KM84), which played an important role during the stabilisation stage, then disappeared from the reactor on Day 188, and again increased slightly to a relative abundance of 0.4% in the deterioration phase. *Methanosarcina thermophila* is capable of slow hydrogenotrophic growth (Lackner et al. 2018), but it is known to prefer acetate and methanol (Zinder and Mah 1979).

5 | Conclusion

This study integrated genome-resolved metagenomics with reactor performance analysis to explore the relationship between microbial community dynamics and reactor function during the startup of thermophilic anaerobic digestion of sewage sludge. Network analysis revealed three distinct microbial subcommunities, each associated with different operational stages. Notably, the microbial assemblage dominant during the stabilisation stage differed from that during peak performance, suggesting that distinct taxa are responsible for thermophilic adaptation versus sustained high-rate digestion. Syntrophic acetate oxidation emerged as a key methanogenic pathway during peak performance, even though the free ammonia concentrations were relatively low (0.04–0.07 gNL⁻¹), with different SAOB and

one key hydrogenotrophic methanogen prevailing. Genome-resolved metagenomics enabled the identification of several novel taxa potentially involved in syntrophic propionate- and acetate oxidation, as well as a dominant methanogen during peak performance that could not be classified at the species level. These findings advance our understanding of the functional roles of microbial taxa under thermophilic conditions and provide a foundation for optimising anaerobic digestion processes.

Author Contributions

Oskar Modin: conceptualization, data curation, formal analysis, resources, writing – original draft, visualization. **Dan Zheng:** formal analysis, visualization, writing – review and editing. **Anna Schnürer:** writing – review and editing. **Ted Lundwall:** investigation, writing – review and editing. **Santiago Elejalde Bolanos:** investigation, writing – review and editing. **Jesper Olsson:** conceptualization, investigation, formal analysis, methodology, resources, funding acquisition, writing – review and editing.

Acknowledgements

This project was funded by K ppalaf rbundet. We thank Mila Harding for her work with reactor operation and measurement of process data and Marie Abadikhah for help with DNA extractions. Part of the bioinformatics work was enabled by resources in projects NAISS 2023/22-884 and NAISS 2023/23-442 provided by the National Academic Infrastructure for Supercomputing in Sweden (NAISS) at UPPMAX, funded by the Swedish Research Council through grant agreement no. 2022-06725.

Conflicts of Interest

The authors declare no conflicts of interest.

Data Availability Statement

The data that support the findings of this study are openly available in NCBI Sequence Read Archive at <https://www.ncbi.nlm.nih.gov/sra>, reference number PRJNA973019.

References

- Abadikhah, M., M. C. Rodriguez, F. Persson, B. M. Wil n, A. Farewell, and O. Modin. 2022. "Evidence of Competition Between Electrogens Shaping Electroactive Microbial Communities in Microbial Electrolysis Cells." *Frontiers in Microbiology* 13: 959211. <https://doi.org/10.3389/fmicb.2022.959211>.
- Ahring, B. K. 1995. "Methanogenesis in Thermophilic Biogas Reactors." *Antonie Van Leeuwenhoek* 67, no. 1: 91–102. <https://doi.org/10.1007/BF00872197>.
- Anantharaman, K., B. Hausmann, S. P. Jungbluth, et al. 2018. "Expanded Diversity of Microbial Groups That Shape the Dissimilatory Sulfur Cycle." *ISME Journal* 12: 1715–1728. <https://doi.org/10.1038/s41396-018-0078-0>.
- Andrews, K. T., and B. K. C. Patel. 1996. "*Fervidobacterium gondwanense* Sp. Nov., a New Thermophilic Anaerobic Bacterium Isolated From Nonvolcanically Heated Geothermal Waters of the Great Artesian Basin of Australia." *International Journal of Systematic and Evolutionary Microbiology* 46: 265–269. <https://doi.org/10.1099/00207713-46-1-265>.
- Angelidaki, I., X. Chen, J. Cui, P. Kaparaju, and L. Ellegaard. 2006. "Thermophilic Anaerobic Digestion of Source-Sorted Organic Fraction of Household Municipal Solid Waste: Start-Up Procedure for Continuously Stirred Tank Reactor." *Water Research* 40: 2621–2628. <https://doi.org/10.1016/j.watres.2006.05.015>.

- Appels, L., J. Baeyens, J. Degrève, and R. Dewil. 2008. "Principles and Potential of the Anaerobic Digestion of Waste-Activated Sludge." *Progress in Energy and Combustion Science* 34: 755–781. <https://doi.org/10.1016/j.pecc.2008.06.002>.
- Asnicar, F., A. M. Thomas, F. Beghini, et al. 2020. "Precise Phylogenetic Analysis of Microbial Isolates and Genomes From Metagenomes Using PhyloPhlAn 3.0." *Nature Communications* 11: 2500. <https://doi.org/10.1038/s41467-020-16366-7>.
- Ben Hania, W., R. Godbane, A. Postec, M. Hamdi, B. Ollivier, and M.-L. Fardeau. 2012. "*Defluviitoga tunisiensis* Gen. Nov., sp. Nov., a Thermophilic Bacterium Isolated From a Mesothermic and Anaerobic Whey Digester." *International Journal of Systematic and Evolutionary Microbiology* 62: 1377–1382. <https://doi.org/10.1099/ijs.0.033720-0>.
- Bengtsson, S., J. Hallquist, A. Werker, and T. Welander. 2008. "Acidogenic Fermentation of Industrial Wastewaters: Effects of Chemostat Retention Time and pH on Volatile Fatty Acids Production." *Biochemical Engineering Journal* 40: 492–499. <https://doi.org/10.1016/j.bej.2008.02.004>.
- Blanco-Míguez, A., F. Beghini, F. Cumbo, et al. 2023. "Extending and Improving Metagenomic Taxonomic Profiling With Uncharacterized Species Using MetaPhlAn 4." *Nature Biotechnology* 41: 1633–1644. <https://doi.org/10.1038/s41587-023-01688-w>.
- Boušková, A., M. Dohányos, J. E. Schmidt, and I. Angelidaki. 2005. "Strategies for Changing Temperature From Mesophilic to Thermophilic Conditions in Anaerobic CSTR Reactors Treating Sewage Sludge." *Water Research* 39: 1481–1488. <https://doi.org/10.1016/j.watres.2004.12.042>.
- Bowers, R. M., N. C. Kyrpides, R. Stepanauskas, et al. 2017. "Minimum Information About a Single Amplified Genome (MISAG) and a Metagenome-Assembled Genome (MIMAG) of Bacteria and Archaea." *Nature Biotechnology* 35: 725–731. <https://doi.org/10.1038/nbt.3893>.
- Braguglia, C. M., A. Gianico, A. Gallipoli, and G. Mininni. 2015. "The Impact of Sludge Pre-Treatments on Mesophilic and Thermophilic Anaerobic Digestion Efficiency: Role of the Organic Load." *Chemical Engineering Journal* 270: 362–371. <https://doi.org/10.1016/j.cej.2015.02.037>.
- Buchfink, B., K. Reuter, and H.-G. Drost. 2021. "Sensitive Protein Alignments at Tree-Of-Life Scale Using DIAMOND." *Nature Methods* 18: 366–368. <https://doi.org/10.1038/s41592-021-01101-x>.
- Campanaro, S., L. Treu, L. M. Rodriguez-R, et al. 2020. "New Insights From the Biogas Microbiome by Comprehensive Genome-Resolved Metagenomics of Nearly 1600 Species Originating From Multiple Anaerobic Digesters." *Biotechnology for Biofuels* 13: 25. <https://doi.org/10.1186/s13068-020-01679-y>.
- Chaumeil, P.-A., A. J. Mussig, P. Hugenholz, and D. H. Parks. 2022. "GTDB-Tk v2: Memory Friendly Classification With the Genome Taxonomy Database." *Bioinformatics* 38: 5315–5316. <https://doi.org/10.1093/bioinformatics/btac672>.
- Chen, S., Y. Zhou, Y. Chen, and J. Gu. 2018. "Fastp: An Ultra-Fast All-In-One FASTQ Preprocessor." *Bioinformatics* 34: i884–i890. <https://doi.org/10.1093/bioinformatics/bty560>.
- Chen, Y.-T., Y. Zeng, H.-Z. Wang, et al. 2020. "Different Interspecies Electron Transfer Patterns During Mesophilic and Thermophilic Syntrophic Propionate Degradation in Chemostats." *Microbial Ecology* 80: 120–132. <https://doi.org/10.1007/s00248-020-01485-x>.
- Cheng, G. B., E. Bongcam-Rudloff, and A. Schnürer. 2025. "Metagenomic Exploration Uncovers Several Novel 'Candidatus' Species Involved in Acetate Metabolism in High-Ammonia Thermophilic Biogas Processes." *Microbial Biotechnology* 18: e70133. <https://doi.org/10.1111/1751-7915.70133>.
- Cheng, L., Q. He, C. Ding, L.-r. Dai, Q. Li, and H. Zhang. 2013. "Novel Bacterial Groups Dominate in a Thermophilic Methanogenic Hexadecane-Degrading Consortium." *FEMS Microbiology Ecology* 85: 568–577. <https://doi.org/10.1111/1574-6941.12141>.
- Daly, S. E., and J.-Q. Ni. 2023. "Characterizing and Modeling Hydrogen Sulfide Production in Anaerobic Digestion of Livestock Manure, Agro-Industrial Wastes, and Wastewater Sludge." *GCB Bioenergy* 15: 1273–1286. <https://doi.org/10.1111/gcbb.13093>.
- Danecek, P., J. K. Bonfield, J. Liddle, et al. 2021. "Twelve Years of SAMtools and BCFtools." *GigaScience* 10: giab008. <https://doi.org/10.1093/gigascience/giab008>.
- De Vrieze, J., A. M. Saunders, Y. He, et al. 2015. "Ammonia and Temperature Determine Potential Clustering in the Anaerobic Digestion Microbiome." *Water Research* 75: 312–323. <https://doi.org/10.1016/j.watres.2015.02.025>.
- Dong, X., J. Dröge, C. von Toerne, S. Marozava, A. C. McHardy, and R. U. Meckenstock. 2016. "Reconstructing Metabolic Pathways of a Member of the Genus *Pelotomaculum* Suggesting Its Potential to Oxidize Benzene to Carbon Dioxide With Direct Reduction of Sulfate." *FEMS Microbiology Ecology* 93: fiw254. <https://doi.org/10.1093/femsec/fiw254>.
- Döring, C., and M. Basen. 2024. "Propionate Production by Bacteroidia Gut Bacteria and Its Dependence on Substrate Concentrations Differs Among Species." *Biotechnology for Biofuels and Bioproducts* 17: 95. <https://doi.org/10.1186/s13068-024-02539-9>.
- Drula, E., M.-L. Garron, S. Dogan, V. Lombard, B. Henrissat, and N. Terrapon. 2021. "The Carbohydrate-Active Enzyme Database: Functions and Literature." *Nucleic Acids Research* 50, no. D1: D571–D577. <https://doi.org/10.1093/nar/gkab1045>.
- Dyksma, S., and C. Gallert. 2019. "Candidatus Syntrophosphaera Thermopropionivorans: A Novel Player in Syntrophic Propionate Oxidation During Anaerobic Digestion." *Environmental Microbiology Reports* 11: 558–570. <https://doi.org/10.1111/1758-2229.12759>.
- Dyksma, S., and C. Gallert. 2022. "Effect of Magnetite Addition on Transcriptional Profiles of Syntrophic Bacteria and Archaea During Anaerobic Digestion of Propionate in Wastewater Sludge." *Environmental Microbiology Reports* 14: 664–678. <https://doi.org/10.1111/1758-2229.13080>.
- Elejalde Bolanos, S. 2022. "High-Loaded Thermophilic Anaerobic Digestion of Mixed Sewage Sludge: A Pilot Study. Master Thesis. Karlstad University, Sweden." <https://urn.kb.se/resolve?urn=urn:nbn:se:kau:diva-88282>.
- Eren, A. M., E. Kiefl, A. Shaiber, et al. 2021. "Community-Led, Integrated, Reproducible Multi-Omics With Anvi'o." *Nature Microbiology* 6: 3–6. <https://doi.org/10.1038/s41564-020-00834-3>.
- Ferrer, I., F. Passos, E. Romero, F. Vázquez, and X. Font. 2024. "Optimising Sewage Sludge Anaerobic Digestion for Resource Recovery in Wastewater Treatment Plants." *Renewable Energy* 224: 120123. <https://doi.org/10.1016/j.renene.2024.120123>.
- Fischer, M., and J. Pleiss. 2003. "The Lipase Engineering Database: A Navigation and Analysis Tool for Protein Families." *Nucleic Acids Research* 31: 319–321. <https://doi.org/10.1093/nar/gkg015>.
- Friedman, J., and E. J. Alm. 2012. "Inferring Correlation Networks From Genomic Survey Data." *PLoS Computational Biology* 8: e1002687. <https://doi.org/10.1371/journal.pcbi.1002687>.
- Fuchs, G., E. Stupperich, and R. K. Thauer. 1978. "Acetate Assimilation and the Synthesis of Alanine, Aspartate and Glutamate in Methanobacterium Thermoautotrophicum." *Archives of Microbiology* 117: 61–66. <https://doi.org/10.1007/BF00689352>.
- Gagliano, M. C., C. M. Braguglia, M. Petruccioli, and S. Rossetti. 2015. "Ecology and Biotechnological Potential of the Thermophilic Fermentative Coprothermobacter spp." *FEMS Microbiology Ecology* 91: fiv018. <https://doi.org/10.1093/femsec/fiv018>.

- Galushko, A., and J. Kuever. 2021. "Smithellaceae." In *Bergey's Manual of Systematics of Archaea and Bacteria*, 1–3. Wiley.
- Ganidi, N., S. Tyrrel, and E. Cartmell. 2011. "The Effect of Organic Loading Rate on Foam Initiation During Mesophilic Anaerobic Digestion of Municipal Wastewater Sludge." *Bioresource Technology* 102: 6637–6643. <https://doi.org/10.1016/j.biortech.2011.03.057>.
- Ge, H., P. D. Jensen, and D. J. Batstone. 2011. "Relative Kinetics of Anaerobic Digestion Under Thermophilic and Mesophilic Conditions." *Water Science and Technology* 64: 848–853. <https://doi.org/10.2166/wst.2011.571>.
- Graham, E. D., J. F. Heidelberg, and B. J. Tully. 2017. "BinSanity: Unsupervised Clustering of Environmental Microbial Assemblies Using Coverage and Affinity Propagation." *PeerJ* 5: e3035. <https://doi.org/10.7717/peerj.3035>.
- Grégoire, P., M.-L. Fardeau, M. Joseph, et al. 2011. "Isolation and Characterization of *Thermanaerotherix daxensis* Gen. Nov., sp. Nov., a Thermophilic Anaerobic Bacterium Pertaining to the Phylum "Chloroflexi", Isolated From a Deep Hot Aquifer in the Aquitaine Basin." *Systematic and Applied Microbiology* 34: 494–497. <https://doi.org/10.1016/j.syapm.2011.02.004>.
- Guo, H., M. J. Oosterkamp, F. Tonin, et al. 2021. "Reconsidering Hydrolysis Kinetics for Anaerobic Digestion of Waste Activated Sludge Applying Cascade Reactors With Ultra-Short Residence Times." *Water Research* 202: 117398. <https://doi.org/10.1016/j.watres.2021.117398>.
- Hagberg, A. A., D. A. Schult, and P. J. Swart. 2008. "Exploring Network Structure, Dynamics, and Function Using NetworkX." In *7th Python in Science Conference (SciPy2008)*, edited by G. Varoquaux, T. Vaught, and J. Millman, 11–15. Scientific Research Publishing.
- Hattori, S., Y. Kamagata, S. Hanada, and H. Shoun. 2000. "*Thermacetogenium phaeum* Gen. Nov., sp. Nov., a Strictly Anaerobic, Thermophilic, Syntrophic Acetate-Oxidizing Bacterium." *International Journal of Systematic and Evolutionary Microbiology* 50: 1601–1609. <https://doi.org/10.1099/00207713-50-4-1601>.
- Honorato, R. V. 2016. "CAZy-Parser a Way to Extract Information From the Carbohydrate-Active enZYmes Database." *Journal of Open Source Software* 1: 53. <https://doi.org/10.21105/joss.00053>.
- Huerta-Cepas, J., F. Serra, and P. Bork. 2016. "ETE 3: Reconstruction, Analysis, and Visualization of Phylogenomic Data." *Molecular Biology and Evolution* 33: 1635–1638. <https://doi.org/10.1093/molbev/msw046>.
- Imachi, H., Y. Sekiguchi, Y. Kamagata, S. Hanada, A. Ohashi, and H. Harada. 2002. "*Pelotomaculum thermopropionicum* Gen. Nov., sp. Nov., an Anaerobic, Thermophilic, Syntrophic Propionate-Oxidizing Bacterium." *International Journal of Systematic and Evolutionary Microbiology* 52: 1729–1735. <https://doi.org/10.1099/00207713-52-5-1729>.
- Jain, C., L. M. Rodriguez-R, A. M. Phillippy, K. T. Konstantinidis, and S. Aluru. 2018. "High Throughput ANI Analysis of 90K Prokaryotic Genomes Reveals Clear Species Boundaries." *Nature Communications* 9: 5114. <https://doi.org/10.1038/s41467-018-07641-9>.
- Javier-López, R., N. Geliashvili, and N.-K. Birkeland. 2024. "Comparative Genomics of Fervidobacterium: A New Phylogenomic Landscape of These Wide-Spread Thermophilic Anaerobes." *BMC Genomics* 25: 1248. <https://doi.org/10.1186/s12864-024-11128-x>.
- Johnson, L. A., and L. A. Hug. 2022. "Cloacimonadota Metabolisms Include Adaptations in Engineered Environments That Are Reflected in the Evolutionary History of the Phylum." *Environmental Microbiology Reports* 14: 520–529. <https://doi.org/10.1111/1758-2229.13061>.
- Jost, L. 2006. "Entropy and Diversity." *Oikos* 113: 363–375. <https://doi.org/10.1111/j.2006.0030-1299.14714.x>.
- Kang, D. D., F. Li, E. Kirton, et al. 2019. "MetaBAT 2: An Adaptive Binning Algorithm for Robust and Efficient Genome Reconstruction From Metagenome Assemblies." *PeerJ* 7: e7359. <https://doi.org/10.7717/peerj.7359>.
- Kato, S., F. Elizabeth, and D. Bowman. 2003. "Effect of Aerobic and Anaerobic Digestion on the Viability of *Cryptosporidium parvum* Oocysts and *Ascaris suum* Eggs." *International Journal of Environmental Health Research* 13: 169–179. <https://doi.org/10.1080/0960312031000098071>.
- Keller, A., B. Schink, and N. Müller. 2019. "Energy-Conserving Enzyme Systems Active During Syntrophic Acetate Oxidation in the Thermophilic Bacterium *Thermacetogenium phaeum*." *Frontiers in Microbiology* 10: 2785. <https://doi.org/10.3389/fmicb.2019.02785>.
- Kirkegaard, R. H., M. S. Dueholm, S. J. McIlroy, et al. 2016. "Genomic Insights Into Members of the Candidate Phylum Hyd24-12 Common in Mesophilic Anaerobic Digesters." *ISME Journal* 10: 2352–2364. <https://doi.org/10.1038/ismej.2016.43>.
- Kjerstadius, H., J. Cour Jansen, J. De Vrieze, S. Haghghatafshar, and Å. Davidsson. 2013. "Hygienization of Sludge Through Anaerobic Digestion at 35, 55 and 60°C." *Water Science and Technology* 68: 2234–2239. <https://doi.org/10.2166/wst.2013.486>.
- Kurth, J. M., H. J. M. Op den Camp, and C. U. Welte. 2020. "Several Ways One Goal—Methanogenesis From Unconventional Substrates." *Applied Microbiology and Biotechnology* 104: 6839–6854. <https://doi.org/10.1007/s00253-020-10724-7>.
- Labatut, R. A., L. T. Angenent, and N. R. Scott. 2014. "Conventional Mesophilic vs. Thermophilic Anaerobic Digestion: A Trade-Off Between Performance and Stability?" *Water Research* 53: 249–258. <https://doi.org/10.1016/j.watres.2014.01.035>.
- Lackner, N., A. Hintersonleitner, A. O. Wagner, and P. Illmer. 2018. "Hydrogenotrophic Methanogenesis and Autotrophic Growth of *Methanosarcina thermophila*." *Archaea* 2018: 4712608. <https://doi.org/10.1155/2018/4712608>.
- Langmead, B., and S. L. Salzberg. 2012. "Fast Gapped-Read Alignment With Bowtie 2." *Nature Methods* 9: 357–359. <https://doi.org/10.1038/nmeth.1923>.
- Li, C., L. Hao, F. Lü, H. Duan, H. Zhang, and P. He. 2022. "Syntrophic Acetate-Oxidizing Microbial Consortia Enriched From Full-Scale Mesophilic Food Waste Anaerobic Digesters Showing High Biodiversity and Functional Redundancy." *MSystems* 7: e22. <https://doi.org/10.1128/mSystems.00339-22>.
- Li, D., C. M. Liu, R. Luo, K. Sadakane, and T. W. Lam. 2015. "MEGAHIT: An Ultra-Fast Single-Node Solution for Large and Complex Metagenomics Assembly via Succinct de Bruijn Graph." *Bioinformatics* 31: 1674–1676. <https://doi.org/10.1093/bioinformatics/btv033>.
- Lienen, T., A. Kleyböcker, W. Verstraete, and H. Würdemann. 2014. "Foam Formation in a Downstream Digester of a Cascade Running Full-Scale Biogas Plant: Influence of Fat, Oil and Grease Addition and Abundance of the Filamentous Bacterium *Microthrix parvicella*." *Bioresource Technology* 153: 1–7. <https://doi.org/10.1016/j.biortech.2013.11.017>.
- Liu, C., L. Ren, B. Yan, L. Luo, J. Zhang, and M. K. Awasthi. 2021. "Electron Transfer and Mechanism of Energy Production Among Syntrophic Bacteria During Acidogenic Fermentation: A Review." *Bioresource Technology* 323: 124637. <https://doi.org/10.1016/j.biortech.2020.124637>.
- Liu, C., W. Wang, N. Anwar, Z. Ma, G. Liu, and R. Zhang. 2017. "Effect of Organic Loading Rate on Anaerobic Digestion of Food Waste Under Mesophilic and Thermophilic Conditions." *Energy & Fuels* 31: 2976–2984. <https://doi.org/10.1021/acs.energyfuels.7b00018>.
- Liu, F., Y. Zhang, Y. Zhang, et al. 2024. "Thermodynamic Restrictions Determine Ammonia Tolerance of Functional Floras During Anaerobic Digestion." *Bioresource Technology* 391: 129919. <https://doi.org/10.1016/j.biortech.2023.129919>.

- Liu, Y., D. L. Balkwill, H. C. Aldrich, G. R. Drake, and D. R. Boone. 1999. "Characterization of the Anaerobic Propionate-Degrading Syntrophs *Smithella propionica* Gen. Nov., sp. Nov. and *Syntrophobacter wolinii*." *International Journal of Systematic Bacteriology* 49, no. 2: 545–556. <https://doi.org/10.1099/00207713-49-2-545>.
- Lundwall, T. 2021. "Thermophilic Anaerobic Digestion of Municipal Wastewater Sludges A Pilot Scale Evaluation With Model Assistance. Master Thesis. Royal Institute of Technology (KTH), Sweden." <https://urn.kb.se/resolve?urn=urn:nbn:se:kth:diva-301609>.
- Manzoor, S., A. Schnürer, E. Bongcam-Rudloff, and B. Müller. 2018. "Genome-Guided Analysis of *Clostridium ultunense* and Comparative Genomics Reveal Different Strategies for Acetate Oxidation and Energy Conservation in Syntrophic Acetate-Oxidising Bacteria." *Genes* 9: 225. <https://doi.org/10.3390/genes9040225>.
- Mercado, J. V., M. Koyama, and K. Nakasaki. 2022. "Short-Term Changes in the Anaerobic Digestion Microbiome and Biochemical Pathways With Changes in Organic Load." *Science of the Total Environment* 813: 152585. <https://doi.org/10.1016/j.scitotenv.2021.152585>.
- Modin, O., R. Liébana, S. Saheb-Alam, et al. 2020. "Hill-Based Dissimilarity Indices and Null Models for Analysis of Microbial Community Assembly." *Microbiome* 8: 132. <https://doi.org/10.1186/s40168-020-00909-7>.
- Narihiro, T., M. K. Nobu, N.-K. Kim, Y. Kamagata, and W.-T. Liu. 2015. "The Nexus of Syntrophy-Associated Microbiota in Anaerobic Digestion Revealed by Long-Term Enrichment and Community Survey." *Environmental Microbiology* 17: 1707–1720. <https://doi.org/10.1111/1462-2920.12616>.
- Nissen, J. N., J. Johansen, R. L. Allesøe, et al. 2021. "Improved Metagenome Binning and Assembly Using Deep Variational Autoencoders." *Nature Biotechnology* 39: 555–560. <https://doi.org/10.1038/s41587-020-00777-4>.
- Nkuna, R., A. Roopnarain, C. Rashama, and R. Adeleke. 2022. "Insights Into Organic Loading Rates of Anaerobic Digestion for Biogas Production: A Review." *Critical Reviews in Biotechnology* 42: 487–507. <https://doi.org/10.1080/07388551.2021.1942778>.
- Olliver, B. M., R. A. Mah, T. J. Ferguson, D. R. Boone, J. L. Garcia, and R. Robinson. 1985. "Emendation of the Genus *Thermobacteroides*: *Thermobacteroides proteolyticus* sp. Nov., a Proteolytic Acetogen From a Methanogenic Enrichment." *International Journal of Systematic and Evolutionary Microbiology* 35: 425–428. <https://doi.org/10.1099/00207713-35-4-425>.
- Olm, M. R., C. T. Brown, B. Brooks, and J. F. Banfield. 2017. "dRep: A Tool for Fast and Accurate Genomic Comparisons That Enables Improved Genome Recovery From Metagenomes Through de-Replication." *ISME Journal* 11: 2864–2868. <https://doi.org/10.1038/ismej.2017.126>.
- Olm, M. R., A. Crits-Christoph, S. Diamond, A. Lavy, P. B. M. Carnevali, and J. F. Banfield. 2020. "Consistent Metagenome-Derived Metrics Verify and Delineate Bacterial Species Boundaries." *MSystems* 5: e19. <https://doi.org/10.1128/mSystems.00731-19>.
- Orellana, E., L. D. Guerrero, C. Davies-Sala, M. Altina, R. M. Pontiggia, and L. Erijman. 2022. "Extracellular Hydrolytic Potential Drives Microbiome Shifts During Anaerobic Co-Digestion of Sewage Sludge and Food Waste." *Bioresour Technol* 343: 126102. <https://doi.org/10.1016/j.biortech.2021.126102>.
- Pan, X., L. Zhao, C. Li, et al. 2021. "Deep Insights Into the Network of Acetate Metabolism in Anaerobic Digestion: Focusing on Syntrophic Acetate Oxidation and Homooacetogenesis." *Water Research* 190: 116774. <https://doi.org/10.1016/j.watres.2020.116774>.
- Parks, D. H., M. Imelfort, C. T. Skennerton, P. Hugenholtz, and G. W. Tyson. 2015. "CheckM: Assessing the Quality of Microbial Genomes Recovered From Isolates, Single Cells, and Metagenomes." *Genome Research* 25: 1043–1055. <https://doi.org/10.1101/gr.186072.114>.
- Patel, B. K., H. W. Morgan, J. Wiegell, and R. M. Daniel. 1987. "Isolation of an Extremely Thermophilic Chemoorganotrophic Anaerobe Similar to *Dictyoglomus thermophilum* From New Zealand Hot Springs." *Archives of Microbiology* 147: 21–24. <https://doi.org/10.1007/BF00492899>.
- Puchol-Royo, R., J. Pascual, A. Ortega-Legarreta, et al. 2023. "Unveiling the Ecology, Taxonomy and Metabolic Capabilities of MBA03, a Potential Key Player in Anaerobic Digestion. bioRxiv." <https://doi.org/10.1101/2023.09.08.556800>.
- Puengrang, P., B. Suraraksa, P. Prommeenate, et al. 2020. "Diverse Microbial Community Profiles of Propionate-Degrading Cultures Derived From Different Sludge Sources of Anaerobic Wastewater Treatment Plants." *Microorganisms* 8: 277. <https://doi.org/10.3390/microorganisms8020277>.
- Rawlings, N. D., A. J. Barrett, P. D. Thomas, X. Huang, A. Bateman, and R. D. Finn. 2017. "The MEROPS Database of Proteolytic Enzymes, Their Substrates and Inhibitors in 2017 and a Comparison With Peptidases in the PANTHER Database." *Nucleic Acids Research* 46, no. D1: D624–D632. <https://doi.org/10.1093/nar/gkx1134>.
- Rossetti, S., M. C. Tomei, P. H. Nielsen, and V. Tandoi. 2005. "Microthrix Parvicella", a Filamentous Bacterium Causing Bulking and Foaming in Activated Sludge Systems: A Review of Current Knowledge." *FEMS Microbiology Reviews* 29: 49–64. <https://doi.org/10.1016/j.femsre.2004.09.005>.
- Ryue, J., L. Lin, F. L. Kakar, E. Elbeshbishy, A. Al-Mamun, and B. R. Dhar. 2020. "A Critical Review of Conventional and Emerging Methods for Improving Process Stability in Thermophilic Anaerobic Digestion." *Energy for Sustainable Development* 54: 72–84. <https://doi.org/10.1016/j.esd.2019.11.001>.
- Satoh, H., M. Odagiri, T. Ito, and S. Okabe. 2009. "Microbial Community Structures and in Situ Sulfate-Reducing and Sulfur-Oxidizing Activities in Biofilms Developed on Mortar Specimens in a Corroded Sewer System." *Water Research* 43: 4729–4739. <https://doi.org/10.1016/j.watres.2009.07.035>.
- Seemann, T. 2014. "Prokka: Rapid Prokaryotic Genome Annotation." *Bioinformatics* 30: 2068–2069. <https://doi.org/10.1093/bioinformatics/btu153>.
- Shin, J., H. M. Jang, S. G. Shin, and Y. M. Kim. 2019. "Thermophilic Anaerobic Digestion: Effect of Start-Up Strategies on Performance and Microbial Community." *Science of the Total Environment* 687: 87–95. <https://doi.org/10.1016/j.scitotenv.2019.05.428>.
- Sieber, C. M. K., A. J. Probst, A. Sharrar, et al. 2018. "Recovery of Genomes From Metagenomes via a Dereplication, Aggregation and Scoring Strategy." *Nature Microbiology* 3: 836–843. <https://doi.org/10.1038/s41564-018-0171-1>.
- Singh, A., A. Schnürer, J. Doling, and M. Westerholm. 2023. "Syntrophic Entanglements for Propionate and Acetate Oxidation Under Thermophilic and High-Ammonia Conditions." *ISME Journal* 17: 1966–1978. <https://doi.org/10.1038/s41396-023-01504-y>.
- Song, Y., J. S. Lee, J. Shin, et al. 2020. "Functional Cooperation of the Glycine Synthase-Reductase and Wood-Ljungdahl Pathways for Autotrophic Growth of *Clostridium drakei*." *Proceedings of the National Academy of Sciences of the United States of America* 117: 7516–7523. <https://doi.org/10.1073/pnas.1912289117>.
- Soutschek, E., J. Winter, F. Schindler, and O. Kandler. 1984. "*Acetomicrobium flavidum*, Gen. Nov., sp. Nov., a Thermophilic, Anaerobic Bacterium From Sewage Sludge, Forming Acetate, CO₂ and H₂ From Glucose." *Systematic and Applied Microbiology* 5: 377–390. [https://doi.org/10.1016/S0723-2020\(84\)80039-9](https://doi.org/10.1016/S0723-2020(84)80039-9).
- Stefanie, J. W. H. O. E., A. Visser, L. W. H. Pol, and A. J. M. Stams. 1994. "Sulfate Reduction in Methanogenic Bioreactors." *FEMS Microbiology Reviews* 15: 119–136. <https://doi.org/10.1111/j.1574-6976.1994.tb00130.x>.

- Steiniger, B., S. Hupfauf, H. Insam, and C. Schaum. 2023. "Exploring Anaerobic Digestion From Mesophilic to Thermophilic Temperatures—Operational and Microbial Aspects." *Fermentation* 9: 798. <https://doi.org/10.3390/fermentation9090798>.
- Sun, W., G. Yu, T. Louie, et al. 2015. "From Mesophilic to Thermophilic Digestion: The Transitions of Anaerobic Bacterial, Archaeal, and Fungal Community Structures in Sludge and Manure Samples." *Applied Microbiology and Biotechnology* 99: 10271–10282. <https://doi.org/10.1007/s00253-015-6866-9>.
- Takács, I., A. E. Stricker, S. Achleitner, A. Barrie, W. Rauch, and S. Murthy. 2008. "Do You Know Your Sludge Age." *Proceedings of the Water Environment Federation* 13: 3639–3655. <https://doi.org/10.2175/193864708788733486>.
- Tezel, U., M. Tandukar, M. G. Hajaya, and S. G. Pavlostathis. 2014. "Transition of Municipal Sludge Anaerobic Digestion From Mesophilic to Thermophilic and Long-Term Performance Evaluation." *Bioresource Technology* 170: 385–394. <https://doi.org/10.1016/j.biortech.2014.08.007>.
- Theuerl, S., J. Klang, M. Heiermann, and J. De Vrieze. 2018. "Marker Microbiome Clusters Are Determined by Operational Parameters and Specific Key Taxa Combinations in Anaerobic Digestion." *Bioresource Technology* 263: 128–135. <https://doi.org/10.1016/j.biortech.2018.04.111>.
- Tian, Z., Y. Zhang, Y. Li, Y. Chi, and M. Yang. 2015. "Rapid Establishment of Thermophilic Anaerobic Microbial Community During the One-Step Startup of Thermophilic Anaerobic Digestion From a Mesophilic Digester." *Water Research* 69: 9–19. <https://doi.org/10.1016/j.watres.2014.11.001>.
- Uritskiy, G. V., J. DiRuggiero, and J. Taylor. 2018. "MetaWRAP—A Flexible Pipeline for Genome-Resolved Metagenomic Data Analysis." *Microbiome* 6: 158. <https://doi.org/10.1186/s40168-018-0541-1>.
- Vanwonterghem, I., P. D. Jensen, K. Rabaey, and G. W. Tyson. 2016. "Genome-Centric Resolution of Microbial Diversity, Metabolism and Interactions in Anaerobic Digestion." *Environmental Microbiology* 18: 3144–3158. <https://doi.org/10.1111/1462-2920.13382>.
- Vasimuddin, M., S. Misra, H. Li, and S. Aluru. 2019. "Efficient Architecture-Aware Acceleration of BWA-MEM for Multicore Systems." In *2019 IEEE International Parallel and Distributed Processing Symposium (IPDPS)*, 314–324. IEEE.
- Virtanen, P., R. Gommers, T. E. Oliphant, et al. 2020. "SciPy 1.0: Fundamental Algorithms for Scientific Computing in Python." *Nature Methods* 17: 261–272. <https://doi.org/10.1038/s41592-019-0686-2>.
- Visser, A., L. W. Hulshoff Pol, and G. Lettinga. 1996. "Competition of Methanogenic and Sulfidogenic Bacteria." *Water Science and Technology* 33: 99–110. [https://doi.org/10.1016/0273-1223\(96\)00324-1](https://doi.org/10.1016/0273-1223(96)00324-1).
- Vu, H. P., L. N. Nguyen, Q. Wang, et al. 2022. "Hydrogen Sulphide Management in Anaerobic Digestion: A Critical Review on Input Control, Process Regulation, and Post-Treatment." *Bioresource Technology* 346: 126634. <https://doi.org/10.1016/j.biortech.2021.126634>.
- Waite, D. W., M. Chuvochina, C. Pelikan, et al. 2020. "Proposal to Reclassify the Proteobacterial Classes Deltaproteobacteria and Oligoflexia, and the Phylum *thermodesulfobacteria* Into Four Phyla Reflecting Major Functional Capabilities." *International Journal of Systematic and Evolutionary Microbiology* 70: 5972–6016. <https://doi.org/10.1099/ijsem.0.004213>.
- Wang, M., H. Chen, and S. Chang. 2024. "Investigation of Volatile Fatty Acids Production in Biological Hydrolysis of Waste Activated Sludge via Microbial Community Network and Fermentation Pathway Analyses." *Journal of Environmental Chemical Engineering* 12: 112056. <https://doi.org/10.1016/j.jece.2024.112056>.
- Wang, X., M. Zhang, Z. Zhou, et al. 2024. "Effect of Extracellular Polymeric Substances Removal and Re-Addition on Anaerobic Digestion of Waste Activated Sludge." *Journal of Water Process Engineering* 57: 104702. <https://doi.org/10.1016/j.jwpe.2023.104702>.
- Watts, S. C., S. C. Ritchie, M. Inouye, and K. E. Holt. 2018. "FastSpar: Rapid and Scalable Correlation Estimation for Compositional Data." *Bioinformatics* 35: 1064–1066. <https://doi.org/10.1093/bioinformatics/bty734>.
- Westerholm, M., M. Calusinska, and J. Dolfing. 2021. "Syntrophic Propionate-Oxidizing Bacteria in Methanogenic Systems." *FEMS Microbiology Reviews* 46: fuab057. <https://doi.org/10.1093/femsre/fuab057>.
- Westerholm, M., S. Isaksson, O. Karlsson Lindsjö, and A. Schnürer. 2018. "Microbial Community Adaptability to Altered Temperature Conditions Determines the Potential for Process Optimisation in Biogas Production." *Applied Energy* 226: 838–848. <https://doi.org/10.1016/j.apenergy.2018.06.045>.
- Westerholm, M., S. Isaksson, L. Sun, and A. Schnürer. 2017. "Microbial Community Ability to Adapt to Altered Temperature Conditions Influences Operating Stability in Anaerobic Digestion." *Energy Procedia* 105: 895–900. <https://doi.org/10.1016/j.egypro.2017.03.408>.
- Westerholm, M., J. Moestedt, and A. Schnürer. 2016. "Biogas Production Through Syntrophic Acetate Oxidation and Deliberate Operating Strategies for Improved Digester Performance." *Applied Energy* 179: 124–135. <https://doi.org/10.1016/j.apenergy.2016.06.061>.
- Wiegant, W. M., M. Hennink, and G. Lettinga. 1986. "Separation of the Propionate Degradation to Improve the Efficiency of Thermophilic Anaerobic Treatment of Acidified Wastewaters." *Water Research* 20: 517–524. [https://doi.org/10.1016/0043-1354\(86\)90202-2](https://doi.org/10.1016/0043-1354(86)90202-2).
- Wijekoon, K. C., C. Visvanathan, and A. Abeynayaka. 2011. "Effect of Organic Loading Rate on VFA Production, Organic Matter Removal and Microbial Activity of a Two-Stage Thermophilic Anaerobic Membrane Bioreactor." *Bioresource Technology* 102: 5353–5360. <https://doi.org/10.1016/j.biortech.2010.12.081>.
- Woodcroft, B. J., S. T. N. Aroney, R. Zhao, et al. 2024. "SingleM and Sandpiper: Robust Microbial Taxonomic Profiles From Metagenomic Data." *bioRxiv*. <https://doi.org/10.1101/2024.01.30.578060>.
- Wu, L., X. Shan, S. Chen, et al. 2020. "Progressive Microbial Community Networks With Incremental Organic Loading Rates Underlie Higher Anaerobic Digestion Performance." *MSystems* 5: 319. <https://doi.org/10.1128/msystems.00357-00319>.
- Wu, Z.-L., Z. Lin, Z.-Y. Sun, M. Gou, Z.-Y. Xia, and Y.-Q. Tang. 2020. "A Comparative Study of Mesophilic and Thermophilic Anaerobic Digestion of Municipal Sludge With High-Solids Content: Reactor Performance and Microbial Community." *Bioresource Technology* 302: 122851. <https://doi.org/10.1016/j.biortech.2020.122851>.
- Xia, Y., Y. Wang, Y. Wang, F. Y. L. Chin, and T. Zhang. 2016. "Cellular Adhesiveness and Cellulolytic Capacity in Anaerolineae Revealed by Omics-Based Genome Interpretation." *Biotechnology for Biofuels* 9: 111. <https://doi.org/10.1186/s13068-016-0524-z>.
- Xu, R., Z.-H. Yang, Y. Zheng, et al. 2018. "Organic Loading Rate and Hydraulic Retention Time Shape Distinct Ecological Networks of Anaerobic Digestion Related Microbiome." *Bioresource Technology* 262: 184–193. <https://doi.org/10.1016/j.biortech.2018.04.083>.
- Yamada, T., H. Imachi, A. Ohashi, et al. 2007. "*Bellilinea caldifistulae* Gen. Nov., sp. Nov. and *Longilinea arvoryzae* Gen. Nov., sp. Nov., Strictly Anaerobic, Filamentous Bacteria of the Phylum Chloroflexi Isolated From Methanogenic Propionate-Degrading Consortia." *International Journal of Systematic and Evolutionary Microbiology* 57: 2299–2306. <https://doi.org/10.1099/ijms.0.65098-0>.
- Yang, P., Y. Peng, H. Tan, et al. 2021. "Foaming Mechanisms and Control Strategies During the Anaerobic Digestion of Organic Waste: A Critical Review." *Science of the Total Environment* 779: 146531. <https://doi.org/10.1016/j.scitotenv.2021.146531>.
- Yang, W., C. Cai, S. Wang, X. Wang, and X. Dai. 2024. "Unveiling the Inactivation Mechanisms of Different Viruses in Sludge Anaerobic Digestion Based on Factors Identification and Damage Analysis."

Bioresource Technology 413: 131541. <https://doi.org/10.1016/j.biortech.2024.131541>.

Zeng, Y., D. Zheng, L.-P. Li, et al. 2024. "Metabolism of Novel Potential Syntrophic Acetate-Oxidizing Bacteria in Thermophilic Methanogenic Chemostats." *Applied and Environmental Microbiology* 90: e23. <https://doi.org/10.1128/aem.01090-23>.

Zhang, L., X. Gong, R. Xu, K. Guo, L. Wang, and Y. Zhou. 2022. "Responses of Mesophilic Anaerobic Sludge Microbiota to Thermophilic Conditions: Implications for Start-Up and Operation of Thermophilic THP-AD Systems." *Water Research* 216: 118332. <https://doi.org/10.1016/j.watres.2022.118332>.

Zhang, Q., J. Hu, D.-J. Lee, Y. Chang, and Y.-J. Lee. 2017. "Sludge Treatment: Current Research Trends." *Bioresource Technology* 243: 1159–1172. <https://doi.org/10.1016/j.biortech.2017.07.070>.

Zhang, Y., C. Li, Z. Yuan, R. Wang, I. Angelidaki, and G. Zhu. 2023. "Syntrophy Mechanism, Microbial Population, and Process Optimization for Volatile Fatty Acids Metabolism in Anaerobic Digestion." *Chemical Engineering Journal* 452: 139137. <https://doi.org/10.1016/j.cej.2022.139137>.

Zinder, S. H., and R. A. Mah. 1979. "Isolation and Characterization of a Thermophilic Strain of Methanosarcina Unable to Use H₂-CO₂ for Methanogenesis." *Applied and Environmental Microbiology* 38: 996–1008. <https://doi.org/10.1128/aem.38.5.996-1008.1979>.

Supporting Information

Additional supporting information can be found online in the Supporting Information section. **Figure S1:** Semi-full scale anaerobic digester system. **Figure S2:** Principal coordinate analysis based on dissimilarity in community composition between samples calculated using Hill-based dissimilarity with diversity order 1. **Figure S3:** Individual VFAs, ammonium and ammonia concentrations, foam index, H₂S fraction in produced gas, and pH in the reactor over time. **Figure S4:** Species-representative genome bins (SGB) belonging to network Module 1 (a), Module 2 (b), and module 3 (c). **Figure S5:** Most abundant taxa with high proportion of hydrolytic genes in their genomes, in module 1 (a–e), module 2 (f–i), and module 3 (j–n). **Figure S6:** Genes in methylmalonyl-CoA pathway for syntrophic propionate oxidation. **Figure S7:** Methylmalonyl-CoA pathway genes detected in bins in Module 1 and in bins that could not be placed in one of the three major network modules. **Figure S8:** Methylmalonyl-CoA pathway genes detected in bins in Module 2. **Figure S9:** Methylmalonyl-CoA pathway genes detected in bins in Module 3. **Figure S10:** Relative abundance of most abundant taxa classified as putative syntrophic propionate oxidising bacteria, in module 1 (a–f), module 2 (g–j), and module 3 (k–n). **Figure S11:** Genes in the Wood-Ljungdahl and glycine cleavage pathways used by acetogens and syntrophic acetate oxidizing bacteria. **Figure S12:** Wood-Ljungdahl and glycine cleavage pathway genes detected in bins in Module 1 and in bins that could not be placed in one of the three major network modules. **Figure S13:** Wood-Ljungdahl and glycine cleavage pathway genes detected in bins in Module 2. **Figure S14:** Wood-Ljungdahl and glycine cleavage pathway genes detected in bins in Module 3. **Figure S15:** Relative abundance of most abundant taxa with the Wood-Ljungdahl and glycine cleavage pathways, in module 1 (a–f), module 2 (g–j), and module 3 (k–n). **Figure S16:** Relative abundance of possible SAOB, in module 2 (a) and 3 (b–e). **Figure S17:** Genes in dissimilatory sulfate reduction. **Figure S18:** Dissimilatory sulfate reduction pathway genes detected in bins in Module 1. **Figure S19:** Dissimilatory sulfate reduction pathway genes detected in bins in Module 2. **Figure S20:** Dissimilatory sulfate reduction pathway genes detected in bins in Module 3. **Figure S21:** Relative abundance of the most abundant putative sulfate reducing bacteria, in Module 1 (a–f), module 2 (g–j), and module 3 (k–n). **Figure S22:** Genes in methanogenic pathways. **Figure S23:** Detection of methanogenesis genes in the SGB. **Figure S24:** Relative abundance of methanogens, in Module 1 (a–g), Module 2 (h–j), and Module 3 (k). **Data S1:** mbt270238-sup-0002-DataS1.xlsx. **Data S2:** mbt270238-sup-0003-DataS2.xlsx.